Multiple Mechanisms Inactivate the LIN-41 RNA-Binding Protein To Ensure a Robust Oocyte-to-Embryo Transition in *Caenorhabditis elegans*

Caroline A. Spike, Gabriela Huelgas-Morales, Tatsuya Tsukamoto, and David Greenstein[1]
Department of Genetics, Cell Biology and Development, University of Minnesota, Minneapolis, Minnesota 55455
ORCID IDs: 0000-0001-5306-3791 (T.T.); 0000-0001-8189-2087 (D.G.)

ABSTRACT In the nematode *Caenorhabditis elegans*, the conserved LIN-41 RNA-binding protein is a translational repressor that coordinately controls oocyte growth and meiotic maturation. LIN-41 exerts these effects, at least in part, by preventing the premature activation of the cyclin-dependent kinase CDK-1. Here we investigate the mechanism by which LIN-41 is rapidly eliminated upon the onset of meiotic maturation. Elimination of LIN-41 requires the activities of CDK-1 and multiple SCF (Skp1, Cul1, and F-box protein)-type E3 ubiquitin ligase subunits, including the conserved substrate adaptor protein SEL-10/Fbw7/Cdc4, suggesting that LIN-41 is a target of ubiquitin-mediated protein degradation. Within the LIN-41 protein, two nonoverlapping regions, Deg-A and Deg-B, are individually necessary for LIN-41 degradation; both contain several potential phosphodegron sequences, and at least one of these sequences is required for LIN-41 degradation. Finally, Deg-A and Deg-B are sufficient, in combination, to mediate SEL-10-dependent degradation when transplanted into a different oocyte protein. Although LIN-41 is a potent inhibitor of protein translation and M phase entry, the failure to eliminate LIN-41 from early embryos does not result in the continued translational repression of LIN-41 oocyte messenger RNA targets. Based on these observations, we propose a model for the elimination of LIN-41 by the SEL-10 E3 ubiquitin ligase and suggest that LIN-41 is inactivated before it is degraded. Furthermore, we provide evidence that another RNA-binding protein, the GLD-1 tumor suppressor, is regulated similarly. Redundant mechanisms to extinguish translational repression by RNA-binding proteins may both control and provide robustness to irreversible developmental transitions, including meiotic maturation and the oocyte-to-embryo transition.

KEYWORDS oocyte meiotic maturation; oocyte-to-embryo transition; translational regulation; RNA-binding proteins; ubiquitin-mediated protein degradation

IN *Caenorhabditis elegans*, as in many animals, full-grown oocytes are transcriptionally quiescent and depend on a maternal load of protein and messenger RNA (mRNA) to complete their development. As a consequence, the dramatic cell cycle and developmental changes that occur during the transition from oogenesis to embryogenesis are driven by post-transcriptional mechanisms. Such mechanisms include protein phosphorylation, the elimination of maternally provided proteins or mRNAs, and the regulation of maternal mRNA translation [reviewed by Verlhac *et al.* (2010), Robertson and Lin (2015), Svoboda *et al.* (2017)]. The oocyte-to-embryo transition (OET) initiates when oocytes exit meiotic prophase and enter the first meiotic metaphase, a cell cycle and developmental event also known as meiotic resumption or meiotic maturation. The OET completes when zygotic gene transcription begins after fertilization in the early embryo.

Pioneering studies using amphibian oocytes established that oocyte meiotic maturation is initiated by the activation of maturation-promoting factor (MPF), in response to progesterone from the follicle cells [Masui and Markert 1971; reviewed by Masui (2001)]. The principal components of MPF are the cyclin-dependent kinase Cdk1 catalytic subunit and a cyclin B regulatory subunit [Dunphy *et al.* 1988; Gautier *et al.* 1988, 1990; Lohka *et al.* 1988; reviewed by

doi: https://doi.org/10.1534/genetics.118.301421
Manuscript received July 26, 2018; accepted for publication September 10, 2018; published Early Online September 11, 2018.
Available freely online through the author-supported open access option.
Supplemental material available at Figshare: https://doi.org/10.25386/genetics.7056557.
[1]Corresponding author: Department of Genetics, Cell Biology, and Development, University of Minnesota, 4-208 MCB, 420 Washington Ave. SE, Minneapolis, MN 55455. E-mail: green959@umn.edu

Nurse (1990)]. In *Xenopus*, which represents the best-studied system from a biochemical standpoint, MPF activation involves the translation of multiple, apparently redundantly acting factors, including the c-mos protein kinase, B-type cyclins, and proteins that remain to be identified [Kobayashi *et al.* 1991; Minshull *et al.* 1991; Nebreda *et al.* 1995; Frank-Vaillant *et al.* 1999; Haccard and Jessus 2006a; reviewed by Haccard and Jessus (2006b)]. Once activated, MPF stimulates multiple positive feedback mechanisms, resulting in the activation of the CDC25 phosphatase, which removes the inhibitory CDK1 phosphorylations at Thr14 and Tyr15 catalyzed by the Wee1 or Myt1 kinases (Kornbluth *et al.* 1994; Mueller *et al.* 1995; Kumagai and Dunphy 1996). This regulatory mechanism generates the "switch-like" activation of MPF that promotes the rapid and irreversible cell cycle transition from prophase to metaphase [reviewed by O'Farrell (2001), Kishimoto (2015)].

MPF is the master regulator of cell cycle progression during oocyte meiotic maturation in *C. elegans* as in all examined species (Boxem *et al.* 1999; Burrows *et al.* 2006; van der Voet *et al.* 2009), yet MPF activation is regulated somewhat differently than in *Xenopus*. For example, the signal that triggers MPF activation for meiotic maturation in *C. elegans* is not progesterone, but rather the major sperm protein, an abundant cytoskeletal protein that is released from sperm (Miller *et al.* 2001; Kosinski *et al.* 2005). The latter control mechanism, which serves to link meiotic maturation and ovulation to sperm availability, likely evolved in gonochoristic predecessors of facultative hermaphroditic nematode species like *C. elegans*. The rate of meiotic maturation declines substantially as a *C. elegans* hermaphrodite utilizes its limited supply of sperm for self-fertilization but rapidly increases upon mating (Kosinski *et al.* 2005). When sperm are absent, as in mutant hermaphrodites that do not produce sperm (*e.g.*, *fog* mutant females), oocytes arrest for prolonged periods and the rate of production and growth of new oocytes declines until insemination (McCarter *et al.* 1999; Wolke *et al.* 2007; Govindan *et al.* 2009). This serves to preserve metabolically costly oocytes when sperm are unavailable for fertilization. Thus, the molecular mechanisms that control MPF activation must be exquisitely fine-tuned for sperm sensing.

Another commonality between the *C. elegans* and *Xenopus* systems is that MPF activation depends on translational control mechanisms, although the details differ. In *C. elegans*, large ribonucleoprotein (RNP) complexes containing the tripartite motif (TRIM)-NHL (NCL-1, HT2A, and LIN-41) RNA-binding protein LIN-41 and the tristetraprolin/TIS11-related RNA-binding proteins OMA-1 and OMA-2 (referred to collectively as the OMA proteins) are major downstream targets of major sperm protein signaling (Spike *et al.* 2014a,b; Tsukamoto *et al.* 2017). LIN-41 is the chief determinant of the extended meiotic prophase of *C. elegans* oocytes (Spike *et al.* 2014a). In *lin-41* null mutants, pachytene-stage oocytes cellularize prematurely, activate CDK-1, aberrantly disassemble the synaptonemal complex, and enter M phase precociously, causing sterility (Spike *et al.* 2014a; Tocchini *et al.* 2014; Matsuura *et al.* 2016). Premature CDK-1 activation causes *lin-41* mutant oocytes to abnormally transcribe and express genes that are ordinarily expressed after the OET and restricted to differentiated cells (Allen *et al.* 2014; Spike *et al.* 2014a; Tocchini *et al.* 2014). In mammals, LIN-41/TRIM71 has been found to promote pluripotency through its activity as a translational repressor (Loedige *et al.* 2013, 2015; Worringer *et al.* 2014). In *C. elegans*, LIN-41 inhibits CDK-1 activation in part through the 3′-untranslated region (UTR)-mediated translational repression of the CDC-25.3 phosphatase (Spike *et al.* 2014a,b). By contrast, the OMA proteins are redundantly required for CDK-1 activation (Detwiler *et al.* 2001). In the absence of the OMA proteins, oocytes fail to undergo meiotic maturation despite the presence of sperm, resulting in sterility (Detwiler *et al.* 2001).

Genetic analysis suggests the OMA proteins promote meiotic maturation by inhibiting the function of LIN-41 in the most proximal oocyte. Two lines of molecular evidence are consistent with the idea that LIN-41 must be inactivated to promote meiotic maturation. First, LIN-41 is degraded upon the onset of meiotic maturation in response to CDK-1 activation (Spike *et al.* 2014a; Figure 1, A and B). Second, LIN-41 is a potent translational repressor, yet several of the mRNAs it associates with and represses are translated and coexpressed with LIN-41 prior to meiotic maturation in the −1 and −2 oocytes (Tsukamoto *et al.* 2017). These mRNAs include those encoding the RNA-binding protein SPN-4, which is required for development of the embryonic germline and the mesendoderm (Gomes *et al.* 2001), and MEG-1, which is a germplasm or P granule component needed for germline development (Leacock and Reinke 2008; Kapelle and Reinke 2011; Wang *et al.* 2014). By contrast, the OMA proteins are required for the translation of *spn-4* and *meg-1* transcripts in proximal oocytes, providing a molecular mechanism by which the OMA proteins might antagonize LIN-41 function (Tsukamoto *et al.* 2017).

Here we examine the mechanism by which LIN-41 is eliminated by the end of the first meiotic division. We identify two LIN-41 degradation domains, Deg-A and Deg-B, and a potential CDK-1 phosphorylation site within Deg-A, each of which is required for efficient degradation. Transplantation of both LIN-41 degradation domains into OMA-2 results in the premature degradation of the resulting fusion protein during meiosis. Furthermore, we find that a Skp, Cullin, and F-box (SCF) E3 ubiquitin ligase complex containing the substrate recognition subunit SEL-10 (referred to as $SCF^{SEL\text{-}10}$) promotes the degradation of LIN-41 and likely functions through the newly identified degradation domains of LIN-41. SEL-10 is a highly conserved F-box protein important for cell cycle regulation in both yeast (cell division control protein 4; Cdc4) and humans (F-box and WD repeat domain protein; FBW7) [reviewed in Deshaies and Ferrell (2001), Welcker and Clurman (2008)]. In *C. elegans*, *sel-10* does not have an essential mitotic cell cycle role but was identified as a negative regulator of LIN-12/Notch signaling (Sundaram and Greenwald 1993; Hubbard *et al.* 1997).

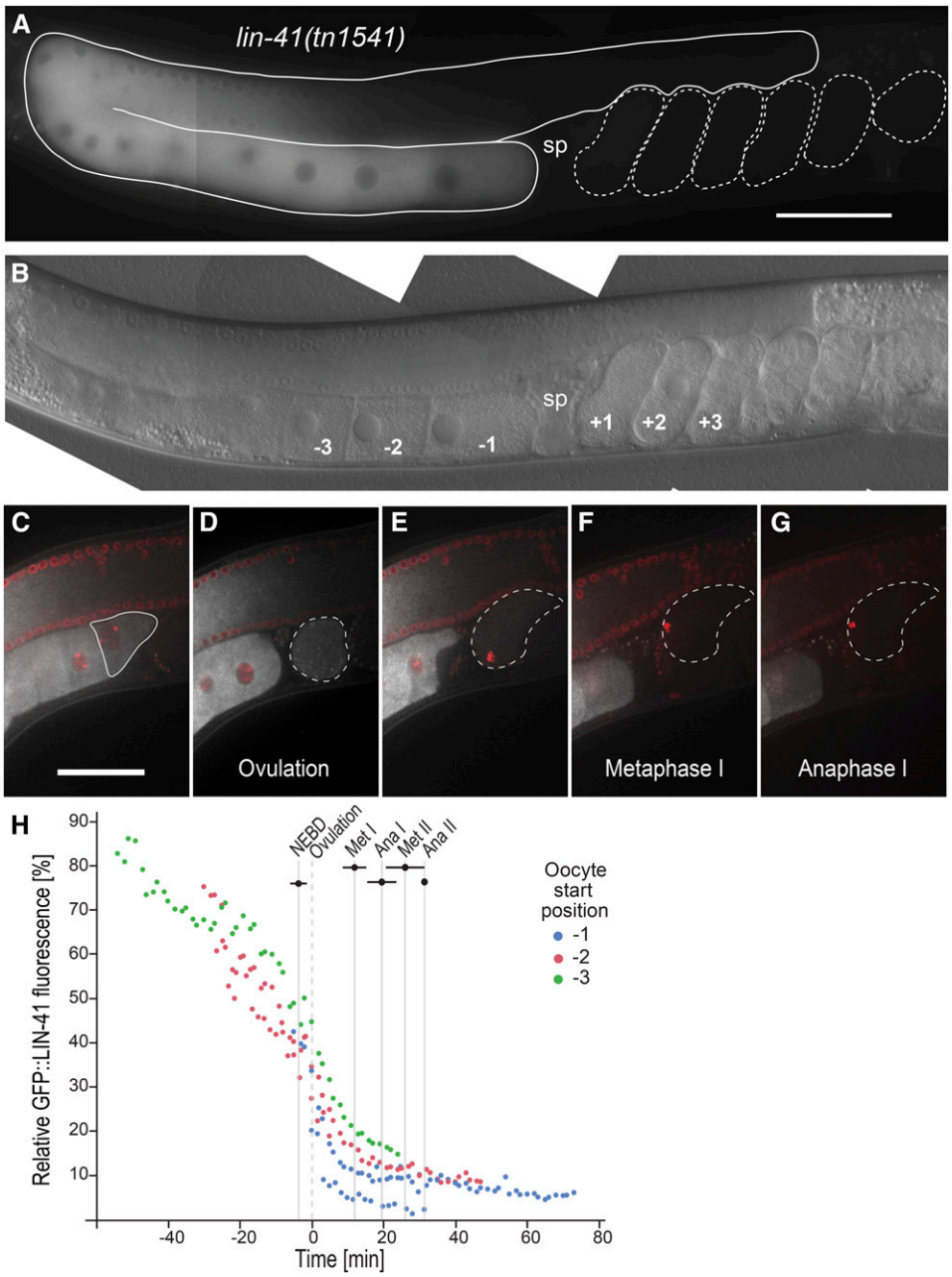

Figure 1 GFP::LIN-41 is eliminated during the first meiotic division. (A and B) Composite GFP (A) and DIC (B) images of a *lin-41*(*tn1541*[*gfp*::*tev*::*s-tag*::*lin-41*]) adult hermaphrodite. GFP::LIN-41 is apparent in the middle and proximal regions of the germline (solid outline, A), with reduced levels in the −1 oocyte immediately adjacent to the spermatheca (sp). The positions of some embryos (dashed outlines, A) and oocytes are indicated relative to the spermatheca in B; a fertilized embryo in the spermatheca would be at the zero position. These labels and naming conventions are used throughout. 100 ms GFP exposures; Bar, 50 μm. (C–G) Time-lapse images of GFP::LIN-41 (white) and mCHERRY::HISTONE-labeled chromosomes (red) were acquired in a living *lin-41*(*tn1541*); *itIs37*[*pie-1p*::*mCherry*::*H2B*::*pie-1 3′UTR*, *unc-119*(+)] adult hermaphrodite by confocal microscopy. Images are shown for select time points (*t*) prior to meiotic maturation (C, *t*= −4.5 min), at ovulation (D, *t* = 0 min), and during the first meiotic division (E, *t*= +4 min; F, *t* = +11.8 min; G, *t*= +16.9 min) as an individual oocyte (C, solid outline) progresses from the −1 to the +1 position and through the OET (D–G, dashed outlines). Bar, 50 μm. Movie S1, worm 1, shows the complete time-lapse series from which the still images were taken. (H) Five oocytes were imaged as they progressed from the −1 position through meiotic divisions; the relative amount of background-corrected GFP::LIN-41 with respect to distal oocytes is shown on the graph at each time point. Three of the oocytes were also imaged at earlier stages as they moved from a more distal location [−2 oocyte (red) or −3 oocyte (green) position] into the −1 oocyte position (blue), as indicated. Timing on the *x*-axis is relative to ovulation (*t* = 0). Bars indicate the SD for different meiotic events. Ana, anaphase; Met, metaphase; NEBD, nuclear envelope breakdown.

Intriguingly, we show that SEL-10 is also important for the degradation of the tumor suppressor protein GLD-1/STAR RNA-binding protein, which is required for oocyte differentiation and represses translation in oocytes (Francis *et al.* 1995a,b; Jones and Schedl 1995; Lee and Schedl 2001; Schumacher *et al.* 2005; Jungkamp *et al.* 2011; Wright *et al.* 2011; Farley and Ryder 2012; Scheckel *et al.* 2012; Doh *et al.* 2013). GLD-1 was independently identified as a target of SEL-10-mediated degradation by Kisielnicka *et al.* (2018) along with CPB-3, a cytoplasmic polyadenylation element-binding protein, which is also important for oocyte development (Boag *et al.* 2005; Hasegawa *et al.* 2006). GLD-1 and CPB-3 are degraded during meiotic prophase, as immature oocytes transition from pachytene to diplotene, considerably earlier than the degradation of LIN-41 during the OET. This variation in timing is due to contrasting mechanisms of signaling-mediated control; while the degradation of LIN-41 is regulated by activated CDK-1 (Spike *et al.* 2014a and this work), the degradation of GLD-1 and CPB-3 is regulated by the mitogen-activated protein (MAP) kinase MPK-1 (Kisielnicka *et al.* 2018 and this work). Contrary to a recent report (Bohnert and Kenyon 2017), we found that the SEL-10-dependent degradation of GLD-1 is not dependent on the presence of sperm in the gonad, contradicting a central aspect of the model proposed by Bohnert and Kenyon (2017) for the regulation of proteostasis renewal during oogenesis. A

surprising finding of our study is that the ectopic expression of LIN-41 and GLD-1 in *sel-10* mutants has only minor effects on fertility and the expression of mRNAs that are translationally repressed by either LIN-41 or GLD-1 during oogenesis. We suggest that the LIN-41 that persists in the embryos of *sel-10* and certain *lin-41* mutants is likely inactivated by additional post-transcriptional mechanisms that remain to be identified.

Materials and Methods

C. elegans strains and phenotypic analysis

Strains: The genotypes of strains used in this study are reported in Supplemental Material, Table S1. The following mutations were used: LGI: *mex-3*(*tn1753*[*gfp*::*3xflag*::*mex-3*]), *air-2*(*or207*ts), *unc-13*(*e1091*), *rrf-1*(*pk1417*), *gld-1*(*q485*), *lin-41*(*tn1487*ts), *lin-41*(*tn1541*[*gfp*::*tev*::*s-tag*::*lin-41*], *lin-41* (*tn1541tn1548*), *lin-41*(*tn1541tn1562*), *lin-41*(*tn1541tn1571*), *lin-41*(*tn1541tn1618*), *lin-41*(*tn1541tn1620*), *lin-41*(*tn1541-tn1622*), *lin-41*(*tn1541tn1628*), *lin-41*(*tn1541tn1630*), *lin-41* (*tn1541tn1635*), *lin-41*(*tn1541tn1638*), *lin-41*(*tn1541tn1641*), *lin-41*(*tn1541tn1643*), *lin-41*(*tn1541tn1645*), *lin-41*(*tn1541-tn1661*), *lin-41*(*tn1541tn1663*), *lin-41*(*tn1541tn1665*), *lin-41* (*tn1541tn1668*), *lin-41*(*tn1541tn1684*), *lin-41*(*tn1541tn1775*), *lin-41*(*tn1767*), *fog-3*(*q470*), and *lin-11*(*n566*); LGIII: *mpk-1* (*ga111*ts), *emb-30*(*tn377*ts), *cdk-1*(*ne2257*ts), *orc-1*(*tn1732* [*mng*::*3xflag*::*orc-1*]), and *cul-2*(*or209*ts); LGIV: *pgl-1*(*sam37* [*pgl-1R765S*::*mTagRFPT*::*3xflag*) (kindly provided by Dustin Updike), *cks-1*(*ne549*ts), and *oma-1*(*zu405te33*). LGV: *spn-4*(*tn1699*[*spn-4*::*gfp*::*3xflag*]), *oma-2*(*te51*), *oma-2*(*cp145* [*mng*::*3xflag*::*oma-2*]), *oma-2*(*tn1760*[*mng*::*3xflag*::*degA*::*oma-2*]), *oma-2*(*tn1764*[*mng*::*3xflag*::*degA*::*degB*::*oma-2*]), *lon-3*(*e2175*), *sel-10*(*ar41*), *sel-10*(*ok1632*), *him-5*(*e1490*), and *fog-2*(*oz40*); and LGX: *meg-1*(*tn1724*[*gfp*::*3xflag*::*meg-1*]). The following rearrangements were used: *hT2*[*bli-4*(*e937*) *let-?*(*q782*) *qIs48*] (I; III) and *nT1*[*qIs51*] (IV; V). The following transgene insertions were used: *axIs1498*[*pie-1p*::*gfp*::*gld-1*::*gld-1 3′UTR*, *unc-119*(+)](Merritt *et al.* 2008), *itIs37*[*pie-1p*::*mCherry*::*H2B*::*pie-1 3′UTR*, *unc-119*(+)] IV (McNally *et al.* 2006), *ozIs5*[*gld-1*::*gfp*] I (kindly provided by Tim Schedl), *ozIs2*[*gld-1*::*gfp*] II (Schumacher *et al.* 2005), and *pwIs116*[*rme-2p*::*rme-2*::*gfp*::*rme-2 3′UTR*, *unc-119*(+)] (Balklava *et al.* 2007).

Phenotypic analysis: Protein expression in living animals or embryos was analyzed using fusions of endogenous loci to green fluorescent protein (GFP; Chalfie *et al.* 1994) or mNeonGreen (mNG; Allele Biotechnology, San Diego, CA; Shaner *et al.* 2013). The persistence of GFP::LIN-41 was evaluated in embryos between the 1- and 12-cell stages located in the spermathecae and uteri of >100 animals. All mutant *lin-41* and *sel-10* alleles with persisting GFP::LIN-41 proteins were fully penetrant. Null mutations in *lin-41* are sterile, with small, abnormal oocytes, and some hypomorphic alleles of *lin-41* affect the production of high-quality oocytes (Slack *et al.* 2000; Spike *et al.* 2014a). Thus, GFP::LIN-41[Δ] was often examined in both heterozygotes (*lin-41*(*tn1541*-Δ)/*unc-13*(*e1091*) *lin-11*(*n566*) genotypes) and homozygotes (*lin-41*(*tn1541*Δ) genotypes), particularly when the *lin-41*(*tn1541*Δ) homozygotes produced obviously small or abnormal oocytes or produced a significant number of dead embryos. All the *sel-10*(*ar41*) strains used also contain *lon-3*(*e2175*), a convenient *cis*-linked marker that encodes a cuticle collagen (Nyström *et al.* 2002; Suzuki *et al.* 2002). The *lon-3*(*e2175*) marker does not affect any of the gene expression patterns reported in this study and was used as a negative control where indicated.

Genome editing

Plasmids capable of expressing guide RNAs (gRNAs) that target the *lin-41* gene were generated as described by Arribere *et al.* (2014) from the vector pRB1017 and sequence-specific oligonucleotides. We estimated the efficiency with which each *lin-41* gRNA was able to target the *lin-41*(*tn1541*) locus by: (1) co-injecting a mixture of the gRNA plasmid (25 ng/μl), the pDD162 plasmid (Dickinson *et al.* 2013), which supplies the Cas9 enzyme (50 ng/μl), and a co-injection marker (*myo-2p*::*Tdtomato*, 4 ng/μl) into *lin-41*(*tn1541*) hermaphrodites; (2) culturing individual F_1 progeny that expressed the co-injection marker (typically ≤10 F_1s from each injected parent); and (3) determining the number of F_1s that segregated F2 progeny with a Dpy *lin-41* loss-of-function (lf) phenotype. File S1 reports the sequences and estimated efficiencies of the gRNAs we used to generate the *lin-41* deletions and point mutations described in this work; most were relatively effective at targeting *lin-41*.

During the efficiency experiments for *lin-41* gRNAs #10 and #11, we identified *lin-41*(*tn1541tn1562*) and *lin-41*(*tn1541tn1571*), respectively, as GFP::LIN-41-positive *lin-41*(*lf*) mutants that appeared to have relatively large deletions by PCR. All of the other deletions were generated in a targeted manner by co-injecting two or more *lin-41* gRNA plasmids (25 ng/μl each), a single-strand oligonucleotide repair template (500 nM), the pDD162 plasmid (50 ng/μl), and a co-injection marker (*myo-2p*::*Tdtomato*, 4 ng/μl) into *lin-41*(*tn1541*) hermaphrodites. We used gRNAs on each side of the desired deletion that, in most cases, would not produce substrates for Cas9 digestion after the deletion event. Otherwise, silent mutations were included in the repair template to prevent recutting. To identify *lin-41*(*tn1541*) deletion mutants, we individually placed F_1 worms expressing the co-injection marker on plates, allowed them to lay eggs, and then used PCR to screen pools of up to six F_1 worms. Pools that appeared to be strongly positive for the desired deletion band were rescreened by PCR to identify F_1 animals that had segregated candidate deletion mutants among their F2 progeny. Mutants were either allowed to become homozygous or were balanced using *hT2*[*bli-4*(*e937*) *let-?*(*q782*) *qIs48*] (I; III). Essentially the same method was used to generate amino acid substitutions in *lin-41*. However,

in those experiments we used only one gRNA and repair events were identified using silent mutations that created restriction enzyme recognition sites in each repair template. Screening therefore consisted of PCR followed by a restriction enzyme digestion, and we only pooled two F_1s in the initial round of screening so that the repair events would be easy to detect. All edited loci were validated by sequencing, and we were able to obtain multiple independent alleles for most targeted deletions and amino acid substitutions. Where possible, two alleles identical to the repair template (but derived from independently injected parents) were saved and assigned allele names. Other, typically imperfect, gene edits were also kept and given allele designations if they were informative or potentially useful. Additional information about all of these alleles and detailed genome-editing information, including gRNA, repair template, and PCR primer sequences, are provided in File S1.

oma-2(*tn1760*) and *oma-2*(*tn1764*) were created using the method described by Dickinson *et al.* (2015) to create *oma-2*(*cp145*). Indeed, we were careful to replicate *oma-2*(*cp145*) as closely as possible; we used the same gRNA plasmid (pDD223) and designed our repair templates to closely mimic pDD271, the repair template used to create *oma-2*(*cp145*). However, instead of using PCR to generate the 3′ homology arms of the repair templates, which contain sequences derived from both *oma-2* and *lin-41*, we synthesized these sequences as gBlocks (Integrated DNA Technologies, Skokie, IL). We minimized the size and complexity of each gBlock by removing introns from the *lin-41*–encoding sequences. *oma-2*(*tn1760*) and *oma-2*(*tn1764*) were perfect matches to the desired repairs (repair templates pCS557 and pCS561, respectively). Gene edited alleles were outcrossed to the wild type before analyzing fertility and embryonic lethality. Specific genome-editing details are provided in File S1.

Microscopy

Movies of GFP::LIN-41, mNG::Deg-A::Deg-B::OMA-2, PGL-1::RFP, and mCHERRY::H2B during the OET were obtained using a Marianas 200 Microscopy Workstation (Intelligent Imaging Innovations, Denver, CO) built on an AxioObserver Z.1 stand (Carl Zeiss, Thornwood, NY), and driven by SlideBook 6.0 software (Intelligent Imaging Innovations). The imaging was performed using a 40× oil Carl Zeiss Plan-Apochromat objective lens (numerical aperture of 1.4) and an Evolve electron-multiplying charge-coupled device camera (Photometrics, Tucson, AZ). Fluorescence intensity quantification from time-lapse images was performed using ImageJ software. All of the other images were acquired on a Carl Zeiss motorized Axioplan 2 microscope with a 63× Plan-Apochromat (numerical aperture 1.4) objective lens, using a AxioCam MRm camera and AxioVision software, version 4.8.2.0 (Carl Zeiss). Image quantifications were performed using the interactive measurements tool in AxioVision to quantify the densitometric mean value of a circumscribed region. The average intensity of SPN-4::GFP fluorescence was measured in a ∼12 μm diameter circle in the anterior cytoplasm of one-cell and two-cell embryos to avoid the bright puncta of SPN-4::GFP in the posterior; these are likely P granules, as SPN-4 is known to associate with these non-membrane-bound organelles in embryos (Ogura *et al.* 2003). The amount of diffusely cytoplasmic SPN-4::GFP appeared to be similar throughout the embryo during these early stages of embryogenesis and in each of the strains we analyzed. Likewise, the average intensity of GFP::MEX-3 and mNG::OMA-2 fluorescence was measured in a ∼10 μm diameter circle in the oocyte cytoplasm. Fluorescence was measured in the oocytes that expressed detectable levels of each fusion protein under our imaging conditions (100 and 120 ms for GFP::MEX-3 and mNG::OMA-2, respectively) and were large enough to fit a ∼10 μm diameter circle in the oocyte cytoplasm. GFP::MEX-3 was detected in four or five proximal oocytes in all strains, consistent with previous observations (Tsukamoto *et al.* 2017). mNG::OMA-2 was detected in five or six proximal oocytes in the *sel-10*(*ar41*) mutants and in seven or more proximal oocytes in the control strain.

RNA interference

Gene-specific RNA interference (RNAi) was performed by feeding *C. elegans* with double-strand RNA (dsRNA)-expressing *Escherichia coli* (Timmons and Fire 1998) at 22°, using the RNAi culture media described by Govindan *et al.* (2006). RNAi clones were obtained from Source BioScience (Nottingham, UK), and the identity of each RNAi clone was verified by DNA sequencing. Exposure to dsRNA-expressing *E. coli* was initiated during the fourth larval stage and GFP::LIN-41 was examined after 1 and 2 days. *cdk-1*(*RNAi*), *skr-1*(*RNAi*), and *sel-10*(*RNAi*) at least partially prevented the elimination of GFP::LIN-41 after 1 day, with completely penetrant phenotypic effects on day 2, while *cul-1*(*RNAi*) only prevented the elimination of GFP::LIN-41 after 2 days of RNAi treatment. All images of RNAi-treated animals were collected on day 2. *cul-1*, *cul-2*, and *cul-3* are important for normal embryonic development. We observed highly penetrant embryonic lethality after treating animals with *cul-1*(*RNAi*) and *cul-3*(*RNAi*). However, the *cul-2*(*RNAi*) clone we used targets the *cul-2* 3′UTR and did not cause embryonic lethality. We therefore examined *lin-41*(*tn1541*); *cul-2*(*or209*ts) adults upshifted to 25° as stage 4 (L4) larvae to assess whether *cul-2* is important for the elimination of GFP::LIN-41 from embryos. We observed that GFP::LIN-41 was eliminated normally from the dead embryos produced by *cul-2*(*or209*ts) parents at the restrictive temperature (n = 71). Postdauer *lin-41*(*tn1541tn1618*) animals [and parallel controls treated with *cdk-1*(*RNAi*)] were examined because strong loss-of-function *lin-41* mutant animals are much healthier when they pass through the dauer stage (Spike *et al.* 2014a).

Western blots

Proteins were separated using NuPage 4–12% Bis-Tris gels or 3–8% Tris-Acetate gels (Invitrogen, Carlsbad, CA) and visualized after Western blotting. Blots were blocked with 5% nonfat dried milk. Primary antibodies used to detect proteins

were affinity-purified rabbit anti-LIN-41 R214 (1:20,000 dilution) (Spike *et al.* 2014a), affinity-purified guinea pig anti-LIN-41 GP49E (1:4000 dilution) (Spike *et al.* 2014a), rabbit anti-GFP NB600-308 (1:4000 dilution; Novus Biologicals, Littleton, CO), and rabbit anti-GLD-1 (1:3000 dilution; kindly provided by Sarah Crittenden and Judith Kimble) (Jan *et al.* 1999). Secondary antibodies used for Western blots were peroxidase-conjugated donkey anti-guinea pig (1:40,000 dilution) (Jackson ImmunoResearch, West Grove, PA) and anti-rabbit (1:5000 dilution) (Thermo Scientific, Waltham, MA) antibodies. Detection was performed using SuperSignal West Femto Maximum Sensitivity Substrate (Thermo Scientific).

Antibody staining

Dissected gonads stained with either the rabbit anti-phosphohistone H3 (Ser10) antibody (1:400 dilution; Millipore, Burlington, MA) or the rabbit anti-RME-2 antibody (1:50 dilution, kindly provided by Barth Grant) (Grant and Hirsh 1999) were fixed in 3% paraformaldehyde for 1 hr, as described (Rose *et al.* 1997). Dissected gonads stained with the rabbit anti-GLD-1 primary antibody (1:150 dilution; Jan *et al.* 1999) were fixed in 1% paraformaldehyde for 10 min with a 5-min postfix step in ice-cold methanol. Primary antibodies were detected using either Cy3-conjugated goat anti-rabbit or Alexa 488-conjugated donkey anti-rabbit secondary antibodies (1:500 dilutions; Jackson ImmunoResearch). For the strong loss-of-function *lin-41*(*tn1541tn1618*) mutant, gonads were dissected from postdauer animals on the first day of adulthood.

Data availability

All strains and newly created alleles (see File S1 and Table S1) are available upon request. The sequences of gRNAs, repair templates, PCR primers, *lin-41* alleles, and *oma-2* alleles are presented in File S1. Plasmids producing gRNAs and those containing repair templates for genome editing are available upon request. All Sanger sequencing files are available upon request. Supplemental material available at Figshare: https://doi.org/10.25386/genetics.7056557.

Results

GFP::LIN-41 is eliminated during the first meiotic division

Germline-expressed LIN-41 is restricted to oogenesis and required to prevent premature M phase entry and to promote growth of developing oocytes (Spike *et al.* 2014a). In the oogenic germlines of adult hermaphrodites, LIN-41 is expressed from midpachytene through subsequent stages of oocyte development, with a notable reduction in LIN-41 levels as oocytes initiate meiotic maturation at the end of oogenesis. Essentially the same pattern is seen in the oocytes of *lin-41*(*tn1541*[*gfp*::*tev*::*s-tag*::*lin-41*]) adult hermaphrodites; these animals carry a *gfp*-tagged allele of *lin-41* and express only GFP-tagged LIN-41 (GFP::LIN-41), yet have essentially wild-type oocyte development and fertility (Figure 1, A and B; Spike *et al.* 2014a). GFP::LIN-41 is always visible in the oocyte immediately adjacent to the spermatheca (−1 oocyte), but is not detectable in most embryos, suggesting that GFP::LIN-41 is eliminated soon after meiotic maturation and ovulation (Figure 1, A and B; Spike *et al.* 2014a). To more precisely determine the stage at which GFP::LIN-41 is eliminated during the OET, we used time-lapse imaging to examine GFP::LIN-41 as oocytes proceed through meiotic maturation, are ovulated into and fertilized in the spermatheca, and complete their meiotic divisions (Movie S1 and Figure 1, C–H). We also imaged several oocytes as they moved into the −1 position from a slightly earlier developmental stage (−2 or −3 oocyte start position). Quantification of these images shows that GFP::LIN-41 levels decline slowly during the late stages of oogenesis and then drop dramatically after nuclear envelope breakdown and ovulation (Figure 1, D and H). As a result, GFP::LIN-41 is essentially undetectable well before the end of the first meiotic division (Figure 1, F and G). During meiotic maturation, the −1 oocyte undergoes a cortical cytoskeletal rearrangement prior to ovulation (McCarter *et al.* 1999). GFP::LIN-41 begins to localize to punctate structures in the oocyte cytoplasm during cortical rearrangement, at the onset of its dramatic disappearance (Movie S1). The nature of these punctate structures is unclear; however, most of them do not exhibit colocalization with PGL-1::RFP and therefore do not appear to be P granules (Figure S1, A–C). Collectively, these observations document that preexisting GFP::LIN-41 in the −1 oocyte is rapidly eliminated during meiosis I in a period of ∼10–15 min, likely as a result of protein degradation. *lin-41* mRNA levels also decline during the OET (∼30-fold decrease in one-cell embryos relative to proximal oocytes; Stoeckius *et al.* 2014), suggesting that mRNA destabilization may prevent the resynthesis of LIN-41 after its elimination during meiosis.

Deg-A and Deg-B are required to eliminate GFP::LIN-41 from embryos

To identify the amino acid sequences of LIN-41 required for its elimination from early embryos, we generated a series of deletions in the coding region of the GFP::LIN-41-expressing *lin-41*(*tn1541*) gene using CRISPR-Cas9-based genome-editing approaches. Collectively, these deletions are predicted to remove 95% of the LIN-41 protein and disrupt all known structural domains of LIN-41 (Figure 2, A and B, and File S1). For each mutant, GFP::LIN-41[Δ] expression was examined to determine whether the deleted portion of LIN-41 is necessary for the elimination of GFP::LIN-41 from embryos (Figure 2, D–F, Figure S2, and Figure S3). This approach enabled us to determine that two nonoverlapping regions in the N-terminal third of LIN-41 are required for its elimination from embryos (Figure 2B). We will refer to these regions as the LIN-41 degradation domains Deg-A and Deg-B. Importantly, GFP::LIN-41[Δ] proteins with deletions affecting the Deg-A or Deg-B domains are expressed in

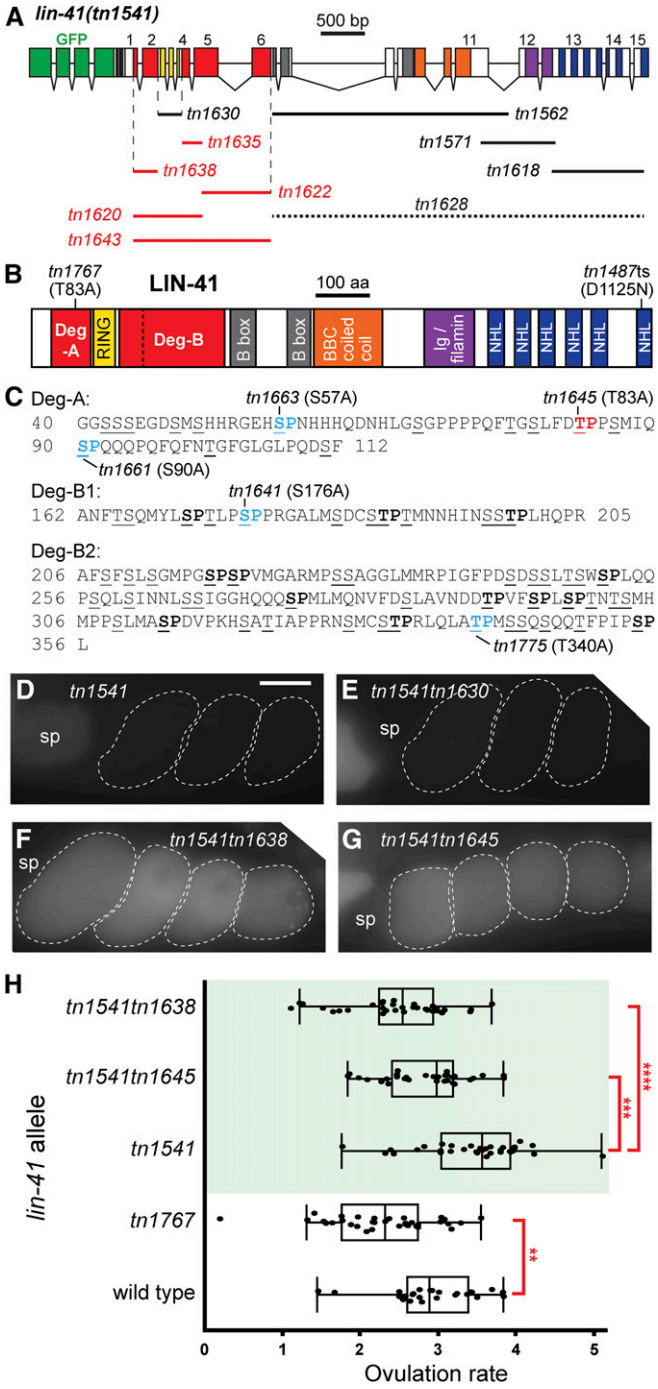

Figure 2 LIN-41 Deg domains are required for the elimination of GFP::LIN-41 upon the onset of meiotic maturation. (A) The exon–intron structure and deletion analysis of *lin-41*(*tn1541*). Colored boxes indicate exonic regions that encode GFP (green) or LIN-41 protein domains (see B). Deletions made in the context of *lin-41*(*tn1541*) are drawn as lines, labeled with a deletion-specific allele name, beneath the LIN-41-encoding exons and introns (exons labeled 1–15). GFP::LIN-41 can be detected in the germline of most deletion mutants (solid lines), with one exception (*tn1628*, dotted line). Deletions in red prevent the elimination of GFP::LIN-41 from early embryos. The vertical dashed lines delimit the beginning of Deg-A and the end of Deg-B, respectively. (B) The previously described [RING (yellow), B-box (gray), BBC (orange), Ig/filamin (purple), NHL (blue)] and newly identified [Deg (red)] protein domains of LIN-41. The vertical dashed line in B indicates the two parts of Deg-B, B1 and B2, which are individually removed in *lin-41*(*tn1541tn1635*) and *lin-41*(*tn1541tn1622*), respectively. The position of two *lin-41* missense alleles (*tn1767*[T83A] and *tn1487*ts[D1125N]) generated in the endogenous *lin-41* locus are indicated. (C) The amino acid sequences of Deg-A, Deg-B1, and Deg-B2. Many of the amino acids are serines and threonines (underlined) and some are potential targets of proline-directed serine/threonine [S/T] kinases (bold). The indicated alleles change an [S/T] residue to an alanine (colored and bold) in the context of *lin-41*(*tn1541*). The *tn1645*[T83A] mutation in Deg-A results in the persistence of GFP::LIN-41[T83A] in embryos (red), whereas the other changes do not (indicated in blue font). (D–G) GFP::LIN-41 is eliminated from the early embryos (dashed outlines) of *lin-41*(*tn1541*) (D, control) and *lin-41*(*tn1541tn1630*) (E, RING deleted) homozygous mutants but persists in the early embryos of *lin-41*(*tn1541tn1638*) (F, Deg-A deleted) and *lin-41*(*tn1541tn1645*) (G, LIN-41[T83A]) homozygous mutants. The position of the spermatheca (sp) is indicated, for reference. 100 ms GFP exposures; Bar, 20 μm. (H) The rate of ovulation is slightly reduced in mutants with a compromised LIN-41 Deg-A domain. Ovulation rate is expressed as the number of ovulations per gonad arm per hr and was measured in at least 25 day 2 adults. The three *gfp*-tagged alleles are in the top portion of the graph with green shading. Significance was determined using a one-way ANOVA test with Tukey's *post hoc* test to compare the means; ** $P < 0.01$, *** $P < 0.001$, and **** $P < 0.0001$. *itIs37*[*pie-1p*::*mCherry*:::*H2B*::*pie-1 3′UTR*, *unc-119*(+)] was also present in each of the GFP::LIN-41-expressing strains; it is not expected to alter the ovulation rate.

proximal oocytes at comparable levels to the wild-type fusion protein (Figure 1 and Figure S2). However, the GFP::LIN-41[ΔDeg] proteins fail to be eliminated upon the onset of meiotic maturation. Sequences similar to Deg-A and Deg-B are found in *Caenorhabditis* nematodes but they appear to be rapidly evolving. In mammalian LIN-41/TRIM71, the region equivalent to Deg-B, which is located between the RING and B-box domains, is predicted to be intrinsically disordered like the *C. elegans* Deg domains (C. Spike and D. Greenstein, unpublished results).

The LIN-41 Deg-A domain is defined by the *lin-41* (*tn1541tn1638*) deletion allele. This deletion is predicted to affect GFP::LIN-41 by removing 73 amino acids on the N-terminal side of the LIN-41 RING domain (Figure 2C and File S1). *lin-41*(*tn1541tn1638*) is immediately adjacent to, but does not overlap, the *lin-41*(*tn1541tn1630*) deletion, which is predicted to affect GFP::LIN-41 by removing the LIN-41 RING finger domain (see File S1 for deleted residues). Consistent with previous amino acid substitution and transgenic rescue data (Tocchini *et al.* 2014), the RING domain is not required for the elimination of GFP::LIN-41 from embryos (Figure 2E and Figure S2). The LIN-41 Deg-B domain is defined by two contiguous, but nonoverlapping, deletions on the C-terminal side of the LIN-41 RING domain. The *lin-41*(*tn1541tn1635*) deletion is predicted to affect GFP::LIN-41 by removing 44 amino acids on the C-terminal side of the LIN-41 RING domain (Deg-B1) (Figure 2C and File S1). Compared to the Deg-A deletion mutant [*lin-41*(*tn1541tn1638*)], the Deg-B1 deletion mutant [*lin-41*(*tn1541tn1635*)] has a relatively low but detectable level of GFP::LIN-41[Δ] in early embryos (compare Figure S2, K and M). However, the *lin-41*(*tn1541tn1622*) deletion (which defines Deg-B2 and the remaining 151 amino acids of Deg-B; Figure 2C and File S1)

has a robust defect in the elimination of GFP::LIN-41[Δ] from early embryos that is apparent in both heterozygous and homozygous deletion mutants (Figure S2, E and G). Finally, deletions predicted to affect GFP::LIN-41 by removing amino acids and structural domains C-terminal to Deg-B were able to eliminate GFP::LIN-41[Δ] from early embryos (Figure 2A and Figure S3). Interestingly, we found that C-terminal domains could only be removed individually or in small groups, as GFP::LIN-41[Δ] was not detectable when a majority of the C terminus was removed [*lin-41*(*tn1541tn1628*) deletion; Figure 2A and Figure S3, M–P].

LIN-41[T83] is required to eliminate LIN-41 from embryos

The results described above indicate that the elimination of GFP::LIN-41 does not depend on any of the previously described structural domains of LIN-41, but instead requires two new regulatory domains. Analysis of the amino acid sequences of Deg-A and Deg-B shows that each regulatory domain contains many possible phosphorylation sites (Figure 2C). Previously published results indicate that the elimination of GFP::LIN-41 from embryos also requires CDK-1 (Spike *et al.* 2014a), a highly conserved, proline-directed, serine/threonine kinase essential for M phase entry during oocyte meiotic maturation in *C. elegans* (Boxem *et al.* 1999). Thus, we hypothesized that LIN-41 might be a direct target of CDK-1 activity, and that phosphorylation of either Deg-A or Deg-B by CDK-1 could be sufficient to trigger the elimination of GFP::LIN-41 from embryos. Eighteen minimal CDK-1 consensus sequences ([S/T]P) are present in Deg-A and Deg-B (Figure 2C), but only a single site, found in Deg-B1, conforms to an expanded CDK1 consensus sequence ([S/T]PX[K/R]) (Ubersax *et al.* 2003). However, changing the potentially phosphorylated residue at this site to an alanine [S176A; *e.g.*, *lin-41*(*tn1541tn1641*)] had no effect on the elimination of GFP::LIN-41 from embryos (Figure 2C and Figure S4A).

Consequently, we shifted our focus to Deg-A, which is relatively small and contains only three potential CDK-1 target sites, but strongly prevents the elimination of GFP::LIN-41 from embryos (Figure S2M). Each site in Deg-A was tested individually to see if it is required for the elimination of GFP::LIN-41 from embryos. Although the mutations S57A and S90A [*e.g.*, *lin-41*(*tn1541tn1663*) and *lin-41*(*tn1541tn1661*), respectively] had no discernable effect (Figure S2C and Figure S4, C and E), the T83A mutation [*e.g.*, *lin-41*(*tn1541tn1645*)] strongly prevented the elimination of GFP::LIN-41 from embryos, similar to the Deg-A deletion mutant (Figure 2G, Figure S2M, and Figure S4G). Time-lapse imaging of oocyte meiotic maturation, ovulation, and fertilization documents that the T83A mutation strongly abrogates the elimination of GFP::LIN-41[T83A] during meiosis I (Movie S2). During cortical rearrangement, GFP::LIN-41[T83A] localized partially to dynamic punctate structures like GFP::LIN-41 (compare Movie S1 and Movie S2); however, unlike the wild-type protein, puncta of GFP::LIN-41[T83A] were also observed during the meiotic divisions. Furthermore, GFP::LIN-41[T83A] persisted through multiple embryonic cleavage divisions and became at least partially associated with P granules by the two-cell stage (Figure S1, D–I and Movie S2). Importantly, total GFP::LIN-41[T83A] levels remain relatively constant throughout the corresponding time period of meiosis, during which GFP::LIN-41 is normally eliminated (compare Movie S1 and Movie S2). These results are consistent with the possibility that phosphorylation of LIN-41 by a proline-directed S/T kinase, such as CDK-1, promotes the rapid degradation of GFP::LIN-41 upon the onset of meiotic maturation. We next replaced T83 with a glutamic acid residue (T83E) [*e.g.*, *lin-41*(*tn1541tn1684*)], which is negatively charged and might function as a phosphomimetic. However, T83E did not result in the premature elimination of GFP::LIN-41, as when CDK-1 is prematurely activated (Spike *et al.* 2014a). Instead, T83E prevented the elimination of GFP::LIN-41 from embryos, similar to T83A (Figure S4, G and I). This result is not unexpected because phosphorylation sites that function to recruit adapter proteins are often not recognized by binding partners after phosphomimetic substitution (Dephoure *et al.* 2013). In fact, phosphomimetic substitutions within recognition domains are known to be ineffective for Fbw7 substrates (Welcker *et al.* 2013), and this is a likely role for the function of T83 and the Deg domains of LIN-41, as we describe below.

A requirement for the extreme N terminus of LIN-41 (amino acids 1–39) with respect to the elimination of GFP::LIN-41 was not examined in the *lin-41*(*tn1541*) deletion analysis. Genetic analysis suggests that this region of LIN-41 is important for downregulating *lin-41* function specifically in the male tail (Del Rio-Albrechtsen *et al.* 2006). Gain-of-function (gf) alleles that affect this part of LIN-41 have a defect in male tail tip retraction, while hermaphrodites appear overtly wild type. *lin-41*(*tn1541*) males also have a male tail tip retraction defect (Figure S5, A and B), suggesting that the GFP tag on the N terminus of LIN-41 disrupts this male-specific function. Furthermore, the amino acid change found in the *lin-41*(*bx37*gf) allele (G35R) does not affect the elimination of GFP::LIN-41 from early embryos [*lin-41*(*tn1541tn1665*); Figure S5, C and E]. For these reasons, we suspect that the extreme N terminus of LIN-41 is unlikely to be involved in the elimination of GFP::LIN-41 from early embryos. One possibility, however, might be that the N-terminal GFP tag on GFP::LIN-41 compromises a function that is required redundantly with Deg-A or Deg-B. To explore this possibility, we generated worms expressing LIN-41[T83A] [*lin-41*(*tn1767*)] and asked whether the untagged protein also persists in embryos. Using Western blots, we found that LIN-41 was undetectable in a lysate made from wild-type embryos, but that LIN-41[T83A] was clearly present in a lysate prepared from *lin-41*(*tn1767*) mutant embryos (Figure S6D). Thus, the T83A mutation abrogates the elimination of both LIN-41 and GFP::LIN-41 from embryos.

Table 1 Fertility and fecundity of *lin-41* alleles at 20°

Genotype	Predicted protein change	Fertile, %[a]	Brood size[b]	Dead embryos, %[c]
lin-41(*tn1541*)	N-terminal GFP	100 (*n* = 68)	316 ± 39[d] (*n* = 6)	0.3 (*n* = 361)
lin-41(*tn1541tn1618*)[e,f]	Δ NHL (AA 819–1128)	1.5 (*n* = 65)	1 (*n* = 1)	ND
lin-41(*tn1541tn1571*)[e,f]	Δ Ig (AA 677–824)	78.5 (*n* = 65)	11 ± 12 (*n* = 9)	57.1[g] (*n* = 35)
lin-41(*tn1541tn1562*)[e,f]	Δ B-box–coiled-coil (AA 356–707)[h]	84 (*n* = 87)	6 ± 3 (*n* = 17)	ND
lin-41(*tn1541tn1643*)[e]	Δ N-terminal (AA 40–356)	66 (*n* = 90)	6 ± 4 (*n* = 48)	75.4[g] (*n* = 142)
lin-41(*tn1541tn1620*)[e]	Δ N-terminal (AA 40–205)	97 (*n* = 67)	39 ± 32 (*n* = 10)	36.4[g] (*n* = 110)
lin-41(*tn1541tn1622*)[e]	Δ Deg-B2 (AA 206–356)	100 (*n* = 65)	33 ± 16 (*n* = 6)	39.0[g] (*n* = 105)
lin-41(*tn1541tn1635*)	Δ Deg-B1 (AA 162–205)	100 (*n* = 70)	127 ± 108 (*n* = 10)	2.9 (*n* = 105)
lin-41(*tn1541tn1630*)	Δ RING (AA 113–161)	98.5 (*n* = 65)	210 ± 87 (*n* = 12)	2.8 (*n* = 144)
lin-41(*tn1541tn1638*)	Δ Deg-A (AA 40–112)	100 (*n* = 70)	217 ± 103 (*n* = 10)	6.3 (*n* = 174)
lin-41(*tn1541tn1645*)	T83A	100 (*n* = 70)	251 ± 86 (*n* = 10)	1.0 (*n* = 193)
lin-41(*tn1767*)	T83A	98.3 (*n* = 120)	313 ± 31 (*n* = 6)	0.0 (*n* = 176)

[a] Fertile animals produced at least one viable offspring.
[b] The average number of progeny that hatched from fertile animals ± SD.
[c] The percent lethality among the embryos laid on day 1 of adulthood.
[d] Essentially identical to the *lin-41*(*tn1541*) brood size previously reported in Spike *et al.* (2014a) (319 ± 28; *n* = 30).
[e] The progeny of *lin-41/hT2*[*qIs48*] hermaphrodites.
[f] These animals have a Dumpy (Dpy) body shape, as previously described for *lin-41*(*lf*) alleles (Slack *et al.* 2000).
[g] Some of the embryos laid were small or otherwise appeared to be abnormal.
[h] The minimum number of amino acids removed by *tn1562*. Assuming the use of an in-frame 5′ splice site in the 17-bp insertion, either one amino acid (L) or five amino acids (LSPLL) would replace amino acids 356–707.

Functional requirements for individual LIN-41 domains

LIN-41 is a large protein with two well-defined domains that are proposed to have strikingly different activities. The first of these is actually the TRIM multidomain arrangement that contains RING, B-box, and coiled-coil domains; many TRIM proteins are thought to function as RING finger E3 ubiquitin ligases (Ikeda and Inoue 2012). The second functional domain is an RNA-binding domain composed of six NHL (NCL-1, HT2A, and LIN-41) repeats at the C terminus of LIN-41 (Slack and Ruvkun 1998; Loedige *et al.* 2015; Kumari *et al.* 2018). Forward and reverse genetic analyses strongly indicate that the NHL domain is important for both the germline and somatic functions of *C. elegans* LIN-41 (Slack *et al.* 2000; Spike *et al.* 2014a; Tocchini *et al.* 2014), consistent with the identification of LIN-41 as a translational repressor in both tissue types (Spike *et al.* 2014b; Aeschimann *et al.* 2017; Tsukamoto *et al.* 2017). By contrast, a deletion of the entire LIN-41 RING domain (Figure 2A), which confers *in vitro* E3 ligase catalytic activity to mouse LIN41 and other TRIM proteins (Rybak *et al.* 2009; Esposito *et al.* 2017), results in appreciable fertility (brood size of 210 ± 87; Table 1) and thus is nonessential for *C. elegans* oogenesis. As described below, the phenotypes seen in *lin-41*(*tn1541*) deletion mutants are consistent with prior observations and provide additional insights into the functions of LIN-41 protein domains.

TRIM (RING, B-box, and coiled-coil) domain: Deletion of the RING finger in the context of GFP::LIN-41 (GFP::LIN-41[ΔRING]) results in only mild defects. Most *lin-41* (*tn1541tn1630*) animals are fertile and have a large number of progeny; no strong defects in oogenesis, embryonic development, or body shape are evident (Table 1 and Figure S2, I and J). We did note, however, that *lin-41*(*tn1541tn1630*) animals appear to be slightly sick and that they produce ~33% fewer progeny than *lin-41*(*tn1541*) hermaphrodites (Table 1). Interestingly, deletion of the other two TRIM sub-domains (GFP::LIN-41[ΔB-box-CC]) causes a much stronger reduction in LIN-41 function. Most (84%) *lin-41* (*tn1541tn1562*) hermaphrodites are fertile, but produce very few progeny (6 ± 4) and have obvious defects in oogenesis as well as a Dumpy (Dpy) body shape (Table 1 and Figure S3, A and B). Thus, *lin-41*(*tn1541tn1562*) is clearly a hypomorphic allele of *lin-41* that affects both its germline and somatic functions.

We note that *lin-41*(*tn1541tn1562*) might remove additional residues beyond the B-box–coiled-coil region because, unlike the other *lin-41*(*tn1541*Δ) mutants we created, *lin-41*(*tn1541tn1562*) is not a precise exon–exon fusion and requires a new in-frame splicing event to make a full-length protein (Figure 2A and File S1). However, the deletion in this mutant was accompanied by the insertion of a small sequence that includes two potential 5′ splice site consensus sequences; both are in-frame with the downstream exon. Furthermore, the relative size of GFP::LIN-41[ΔB-box-BBC] on SDS-PAGE Western blots is consistent with what we expect to see for the protein made by this particular deletion mutant (Figure S6B and File S1). This is also true for the other GFP::LIN-41[Δ] proteins detected using either anti-LIN-41 or anti-GFP antibodies (Figure S6, A–C).

IG/filamin domain: IG/filamin (IG) domains are only found in a subset of TRIM-NHL proteins; structural analysis of this part of *C. elegans* LIN-41 suggests that it forms a classic IG-like domain fold (Tocchini *et al.* 2014). The IG domain has been proposed to function, along with the coiled-coil domain, as a binding platform for proteins that repress the translation of NHL-bound target mRNAs (Loedige *et al.* 2013). *lin-41*(*ma104*) is a hypomorphic allele that likely disrupts the

structure and function of the LIN-41 IG domain (Tocchini *et al.* 2014). As previously reported (Spike *et al.* 2014b), outcrossed *lin-41*(*ma104*) mutant hermaphrodites have mild oocyte defects and a reduced, but still substantial, brood size of 181 progeny (n = 12). Deletion of the IG domain in the context of GFP::LIN-41 (GFP::LIN-41[ΔIG]) results in stronger defects. Most *lin-41*(*tn1541tn1571*) hermaphrodites are fertile, with a very low brood size (11 progeny) and obvious defects in oogenesis (Figure S3, C and D and Table 1). Both alleles also result in worms with an obviously Dpy body shape. Thus, despite the difference in brood size, the alleles that affect the IG domain are hypomorphic and reduce both the germline and somatic functions of *lin-41*. Indeed, it is potentially misleading to conclude that the relative severities of *lin-41*(*ma104*) and *lin-41*(*tn1541tn1571*) are meaningful, as LIN-41 function may be slightly compromised in the *lin-41*(*tn1541*) mutant despite its wild-type brood size (316 ± 39; Table 1; Spike *et al.* 2014a). For example, the introduction of the LIN-41[D1125N] amino acid change in the sixth NHL repeat (Figure 2B) that results in a temperature-sensitive (ts) phenotype in an otherwise wild-type LIN-41 protein [*e.g.*, *lin-41*(*tn1487*(ts); 100% fertile at 15° (n = 224), average brood size of 104 (n = 64); Spike *et al.* 2014a] results in a stronger, but still hypomorphic, phenotype in a GFP::LIN-41 mutant background [*e.g.*, *lin-41*(*tn1541tn1548*); 71% fertile at 15° (n = 21), average brood size of three (n = 15)].

The NHL domain: Deletion of the C-terminal NHL domain in the context of GFP::LIN-41 (GFP::LIN-41[ΔNHL]) results in a strong loss-of-function *lin-41* phenotype. Whereas *lin-41*(*tn1541*) hermaphrodites are fertile, with normal oocyte development and overall appearance, nearly all (98.5%) *lin-41*(*tn1541tn1618*) hermaphrodites are sterile and have a Dpy body shape (Table 1). Oogenesis is extremely abnormal in most animals (Figure S3, G and H), although *lin-41*(*tn1541tn1618*) hermaphrodites produce embryos on occasion (Figure S3, I and J and Table 1). The fact that deletion of the LIN-41 NHL domain does not result in 100% sterility is surprising because the *lin-41*(*n2914*) null mutation has never been observed to produce progeny. Thus, LIN-41 can exhibit some, albeit very low, biological function in the absence of the NHL domain. We suggest that this low-level function may be mediated through components of the LIN-41 RNP (Spike *et al.* 2014b; Tsukamoto *et al.* 2017). We confirmed that CDK-1 exhibits premature activation in *lin-41*(*tn1541tn1618*) mutants, as it does in *lin-41*(*n2914*) null mutants, by staining adult hermaphrodite germlines with an antibody specific to histone H3 phosphorylated on Serine 10 (pH3(S10)). This antibody stains the nucleoplasm and condensed chromosomes of wild-type diakinesis-stage oocytes as they prepare to enter M phase near the spermatheca (Hsu *et al.* 2000). Both M phase and anti-pH3(S10) staining occur prematurely in strong loss-of-function *lin-41* mutants and are *cdk-1*-dependent (Spike *et al.* 2014a). As expected for a strong loss-of-function mutant, and consistent with the idea that premature M phase entry and CDK-1 activation occur prematurely, we detected pH3(S10)-positive condensed chromosomes in or near the loop region of the gonad, and just after the end of pachytene, in most *lin-41*(*tn1541tn1618*) oogenic germlines (n = 6/9). Interestingly, GFP::LIN-41[ΔNHL] forms abnormal aggregates in the oocytes of *lin-41*(*tn1541tn1618*) homozygotes; these aggregates are not seen in heterozygotes (Figure S3, G, I, and K). The reason for this aberrant pattern of localization is unknown, but GFP::LIN-41[ΔNHL] aggregation is also seen in *lin-41*(*tn1541tn1618*); *cdk-1*(*RNAi*) animals (n = 32), and therefore does not depend on the dysregulation of *cdk-1* function that occurs during oogenesis in strong loss-of-function *lin-41* mutants (Spike *et al.* 2014a). These aggregates may reflect abnormal biogenesis of LIN-41 RNPs in the absence of the NHL domain.

Meiotic degradation domains are nonessential: We initially hypothesized that the deletion of LIN-41 degradation domains might result in a gain-of-function phenotype that would affect fertility or embryonic viability. However, *lin-41*(*tn1541tn1643*), a large deletion that removes Deg-A, the RING finger, and Deg-B in the context of GFP::LIN-41, behaves as a recessive hypomorph that preferentially affects germline function. Homozygous mutants do not have a strong Dpy phenotype, but do have an extremely small brood size and display obvious defects in oogenesis and embryogenesis (Figure S2, O and P and Table 1). In contrast, heterozygous *lin-41*(*tn1541tn1643*) mutants appear essentially normal (n = 20). This is also true for deletions that subdivide the large N-terminal region of LIN-41, such as *lin-41*(*tn1541tn1620*) and *lin-41*(*tn1541tn1622*) (Figure S2, A–H and Table 1). Indeed, even when homozygous, the relatively small Deg-A deletion [*lin-41*(*tn1541tn1638*)], which results in abundant GFP::LIN-41[ΔDeg-A] in early embryos, appears to have minimal consequences for GFP::LIN-41 function at 20° (Figure S2, M and N and Table 1). Likewise, animals expressing LIN-41[T83] and GFP::LIN-41[T83] appear essentially wild type; the latter have only a slightly reduced brood size relative to GFP::LIN-41-expressing controls (Figure S4, G and H and Table 1). Consequently, we decided to look carefully at the ovulation rates of the minimally affected LIN-41 Deg-A deletion [*lin-41*(*tn1541tn1638*)] and T83A point mutants [*lin-41*(*tn1541tn1645*) and *lin-41*(*tn1767*)]. Oocyte meiotic maturation is a rate-limiting step for hermaphrodite fertility and the ovulation rate approximates the rate of oocyte meiotic maturation (McCarter *et al.* 1999; Miller *et al.* 2001; Govindan *et al.* 2006). Importantly, several aspects of nuclear and cytoplasmic oocyte maturation occur prematurely in *lin-41*(*lf*) mutations (Spike *et al.* 2014a,b; Tsukamoto *et al.* 2017). Deg-A domain mutants exhibit mean ovulation rates that are significantly reduced relative to genotype-matched controls (Figure 2H). Interestingly, the mean ovulation rate of the *lin-41*(*tn1541*) control strain was elevated relative to wild-type animals (Figure 2H, 3.4 *vs.* 2.9 ovulations per gonad arm per hr). Together, these observations suggest: (1) *lin-41*(*tn1541*) might be a weak hypomorph that causes a slight increase in the oocyte

maturation rate; and (2) Deg-A domain mutants cause the opposite phenotype, a reduced oocyte maturation rate. These changes in the rate of oocyte maturation are relatively modest, however, and our phenotypic analyses generally suggest that the elimination of LIN-41 from early embryos is not a critical control point for regulating LIN-41 function or activity levels *in vivo*.

LIN-41[Deg] domains are sufficient for degradation

OMA-1 and OMA-2 (OMA-1/2) are functionally redundant, cytoplasmic RNA binding proteins expressed in oocytes and early embryos (Detwiler *et al.* 2001) that copurify with LIN-41 RNP complexes (Spike *et al.* 2014b; Tsukamoto *et al.* 2017). OMA-1/2 levels remain high in one-cell embryos until the first mitotic division, when they are rapidly degraded (Lin 2003; Nishi and Lin 2005; Shirayama *et al.* 2006; Stitzel *et al.* 2006). The expression and subsequent elimination of OMA-2 can be easily visualized in *oma-2*(*cp145*) mutants (Dickinson *et al.* 2015; Figure 3A and Figure S7, A and B), which express an mNG-tagged form of OMA-2 that is largely functional *in vivo* [Table 2, compare *oma-1*(*zu405te33*); *oma-2*(*cp145*) to *oma-1*(*zu405te33*); *oma-2*(*te51*)]. We decided to test whether the LIN-41 Deg domains are sufficient to induce the premature degradation of mNG::OMA-2 during meiosis. Molecularly, we placed LIN-41 Deg domains between mNG and OMA-2 (Figure 3, A–C), as this is similar to their locations in GFP::LIN-41 (Figure 2, A and B) and no structural (*e.g.*, X-ray crystallographic) data are available to aid the experimental design. We generated two new *oma-2* alleles that also contain *lin-41*-encoded Deg domains and examined the pattern of mNG::Deg::OMA-2 accumulation prior to the first mitotic division (Figure 3 and Figure S7).

We began by testing LIN-41 Deg-A, which contains T83, the potential CDK-1 target site required for the elimination of LIN-41. *oma-2*(*tn1760*) mutants express mNG::Deg-A::OMA-2 in oocytes and one-cell embryos. Similar to mNG::OMA-2, this protein is present in one-cell embryos just prior to the first mitotic division, but is eliminated from older embryos (Figure 3, D and E, and Figure S7, A, B, E, and F). However, we did note that the amount of mNG fluorescence in older one-cell pronuclear stage embryos was reduced 36% in *oma-2*(*tn1760*) embryos compared to *oma-2*(*cp145*) controls (compare Figure 3, D and E, and Figure S8A). This reduction might be caused by Deg-A-mediated destabilization of the mNG::OMA-2 fusion protein (see below), but is not equivalent to the rapid elimination of GFP::LIN-41 that occurs in meiosis I (Movie S1 and Figure 1). Because Deg-A on its own was not sufficient to trigger the rapid elimination of mNG::OMA-2 from one-cell embryos, we tested LIN-41 Deg-A and Deg-B together. *oma-2*(*tn1764*) mutants express mNG::Deg-A, Deg-B::OMA-2 in oocytes, but in one-cell embryos the amount of mNG fluorescence is substantially reduced or absent (Figure 3F and Figure S7, G and I). To more precisely determine the stage at which mNG::Deg-A, Deg-B::OMA-2 is eliminated, we used time-lapse imaging (Figure 3, L–O and Movie S3). Levels of this fusion protein drop by ~50% during the first meiotic division (Figure 3, M and N) and become essentially undetectable before the end of the second meiotic division (Figure 3O). We conclude that Deg-A and Deg-B are sufficient in combination to trigger the rapid degradation of mNG::OMA-2 during meiosis, although this event is temporally delayed relative to GFP::LIN-41 (Figure 3P).

oma-1 and *oma-2* share redundant functions during both oocyte and early embryo development (Detwiler *et al.* 2001; Guven-Ozkan *et al.* 2008). Double mutants carrying strong loss-of-function alleles [*e.g.*, *oma-1*(*zu405te33*); *oma-2*(*te51*)] are sterile with a defect in meiotic maturation (Detwiler *et al.* 2001; Table 1). For the most part, the embryonic functions of *oma-1/2* have been studied using conditions that reduce, but do not eliminate, OMA-1/2 function in embryos, such as double RNAi or reduction-of-function alleles that are incompletely sterile (Nishi and Lin 2005; Guven-Ozkan *et al.* 2008). In *oma-1*(*zu405te33*); *oma-2*(*tn1764*) double mutants, OMA-2 is expressed during oogenesis but eliminated prematurely from embryos. Consequently, these double mutants are very fertile but produce ~249 progeny that die during embryogenesis (Table 2). Thus, as a novel allele that specifically reduces embryonic OMA-2, *oma-2*(*tn1764*) may be useful for studying the embryonic functions of *oma-1/2*. Our initial observations indicate that young *oma-1*(*zu405te33*); *oma-2*(*tn1764*) embryos exhibit cell division defects and ectopic cleavage furrows (Figure S8B); similar defects have been reported after *oma-1/2*(*RNAi*) depletion (Li *et al.* 2009).

When combined with *oma-1*(*zu405te33*), *oma-2*(*tn1764*) exhibits a stronger embryonic phenotype than either *oma-2*(*cp145*) or *oma-2*(*tn1760*). However, the severity of the *oma-1*(*te33zu405*); *oma-2*(*tn1760*) double-mutant phenotype relative to *oma-1*(*te33zu405*); *oma-2*(*cp145*) was surprising (Table 2; 60% *vs.* 12% embryonic lethality). One possibility for the increased severity of the *oma-1*(*te33-zu405*); *oma-2*(*tn1760*) double-mutant embryonic phenotype might be the reduction in mNG::Deg-A::OMA-2 levels observed in *oma-2*(*tn1760*) pronuclear-stage embryos (Figure 3E and Figure S8A). We examined this more closely by crossing each mNG-tagged *oma-2* allele into an *emb-30*(*tn377*ts) mutant background. *emb-30* encodes a subunit of the Anaphase Promoting Complex (APC), and adult *emb-30*(*tn377*ts) hermaphrodites upshifted to a restrictive temperature (25°) produce one-cell embryos that arrest in the metaphase of the first meiotic division (Furuta *et al.* 2000). Arrest in meiotic metaphase does not prevent or delay the elimination of GFP::LIN-41, which is independent of APC function (Spike *et al.* 2014a). We observed that mNG::OMA-2 is turned over in arrested meiotic embryos, but could typically be seen in four embryos in the uterus of *emb-30*(*tn377ts*); *oma-2*(*cp145*) hermaphrodites after a 5–7 hr upshift to 25° (Figure S8C). In contrast, both of the LIN-41 Deg domain-containing OMA-2 proteins appeared to be less stable under the same conditions. mNG::Deg-A, Deg-B::OMA-2 was seen in 0–1 mNG-positive embryos and appeared to be the

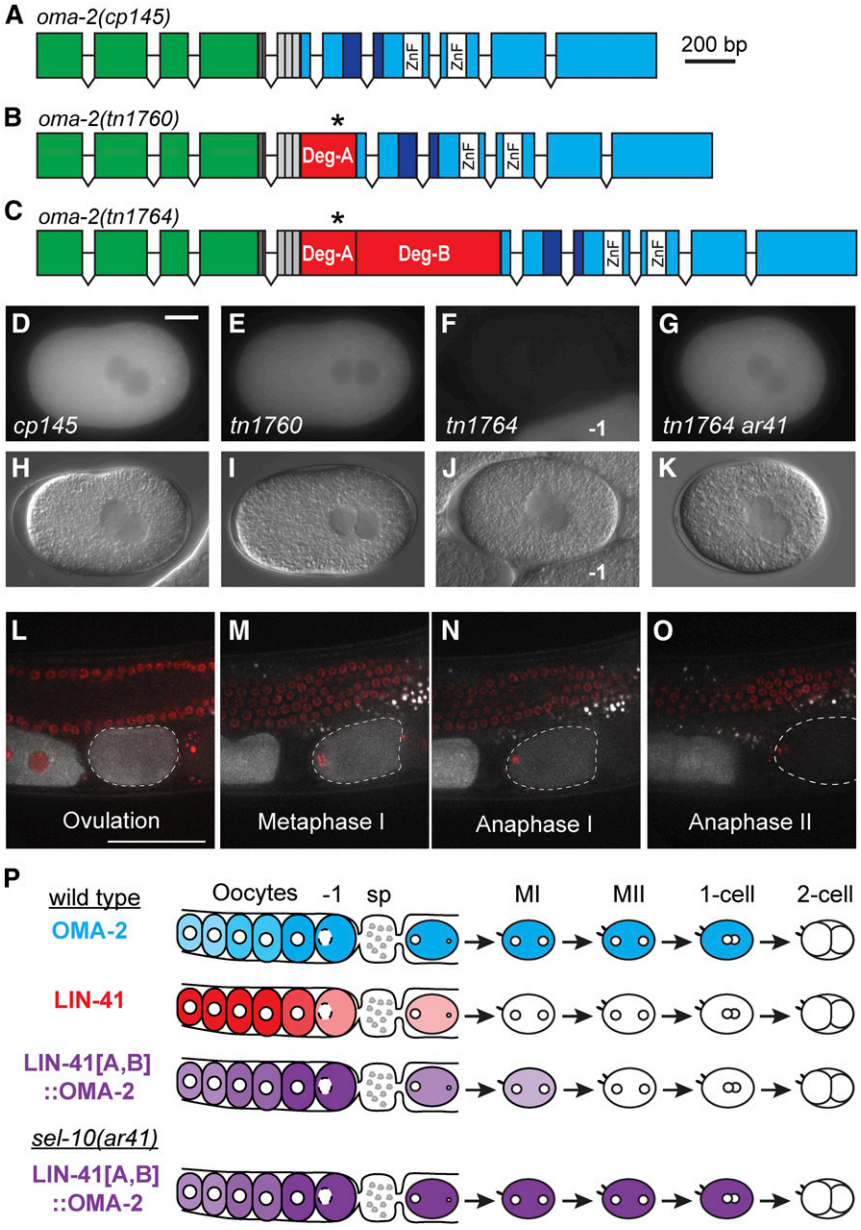

Figure 3 LIN-41 degradation domains when implanted into mNG::OMA-2 promote its rapid elimination during meiosis. (A–C) The exon–intron structures of *oma-2*(*cp145*[*mng*::*tev*::*3xflag*::*oma-2*]), *oma-2*(*tn1760*[*mng*::*tev*::*3xflag*::*deg-a*::*oma-2*]), and *oma-2*(*tn1764*[*mng*::*tev*::*3xflag*::*deg-a*::*deg-b*::*oma-2*]). Boxes represent exonic regions that encode mNeonGreen (green), the tobacco etch virus cleavage site (TEV; dark gray), FLAG epitope tags (light gray), LIN-41 Deg-A and Deg-B domains (red), the likely TAF-4 interaction domain of OMA-2 (dark blue), two OMA-2 CCCH zinc fingers (white), and other OMA-2 coding sequences (cyan). The position of LIN-41 T83 within the LIN-41 Deg-A domain is indicated by an asterisk. (D–K) GFP (D–G) and DIC (H–K) images of *oma-2*(*cp145*) (D and H), *oma-2*(*tn1760*) (E and I), *oma-2*(*tn1764*) (F and J), and *oma-2*(*tn1764*) *lon-3*(*e2175*) *sel-10*(*ar41*) (G and K) one-cell embryos at pronuclear meeting (E and I), or just slightly later, as the pronuclei begin a counterclockwise rotation (D, F–G, H, J, and K) prior to nuclear envelope breakdown and the first mitotic division. Part of a −1 oocyte is visible in F and J, and is indicated for reference. 150 ms GFP exposures; Bar, 10 μm. (L–O) Time-lapse images of mNG::Deg-A,B::OMA-2 (white) and mCHERRY::HISTONE-labeled chromosomes (red) were acquired in a living *oma-2*(*tn1764*); *itIs37*[*pie-1p*::*mCherry*::*H2B*::*pie-1 3′UTR*, *unc-119*(+)] adult hermaphrodite by confocal microscopy. Images are shown for select time points (*t*) at ovulation (L, *t* = 0 min), during the first (M, *t* = +5 min; N, *t* = +10.5 min) and second meiotic divisions (O, *t* = +24.5 min) as an embryo (dashed outline) progresses through both meiotic divisions. See Movie S3 for the complete time-lapse sequence. Bar, 50 μm. (P) A visual summary of the dynamic expression patterns of mNG::OMA-2 (cyan), GFP::LIN-41 (red), and mNG::Deg-A,B::OMA-2 (purple). Oocytes are to the left and embryos are to the right of the spermatheca (sp). Meiotic embryos (MI, MII) have completed their respective divisions.

least stable (Figure S8E), as expected from our previous analysis (Figure 3 and Figure S7). mNG::Deg-A::OMA-2 was seen in two mNG-positive embryos and therefore appeared to be of intermediate stability (Figure S8D). Thus, although Deg-A is not sufficient for rapid elimination, it may reduce the stability of mNG::Deg-A::OMA-2 in meiotic embryos. The consequent reduction in protein levels could contribute to the enhanced severity of the *oma-1*(*te33zu405*); *oma-2*(*tn1760*) double-mutant embryonic phenotype. It is also possible that insertion of LIN-41 Deg-A at the N terminus of OMA-2 might perturb the nearby TAF-4-binding domain (Figure 3, A–C), which is critical for the function of OMA-2 in embryos (Guven-Ozkan *et al.* 2008). It is important to note that OMA-1 proteins with deletions in the TAF-4-binding domain are stable in one-cell embryos (Guven-Ozkan *et al.* 2008) and this is expected to be true for OMA-2. Therefore, we conclude that Deg-A by itself can confer destabilization activity to OMA-2, albeit less potent than that conferred by Deg-A and Deg-B in combination.

GFP::LIN-41 is eliminated from embryos by the SCF^{SEL-10} E3 ubiquitin ligase

Several different SCF-containing E3 ubiquitin ligase complexes promote protein degradation during meiosis and early embryogenesis in *C. elegans* (Peel *et al.* 2012; Du *et al.* 2015; Beard *et al.* 2016). We initially used RNAi to knock down the functions of each of the six cullins identified in the *C. elegans* genome (Kipreos *et al.* 1996; Nayak *et al.* 2002) to determine whether an SCF-type E3 ligase is involved in the elimination of GFP::LIN-41. In general, RNAi was initiated in *lin-41*(*tn1541*) hermaphrodites at the L4 larval stage and GFP::LIN-41 was examined in adults, 2 days after the

Table 2 Sterility and embryonic lethality in *oma-2* and *oma-1*; *oma-2* mutant strains at 20°

Genotype	Embryos laid[a]	Dead embryos, %
oma-2(*cp145*)	314 ± 48 (*n* = 6)	0.6 (*n* = 1793)
oma-2(*tn1760*)	306 ± 39 (*n* = 6)	0.6 (*n* = 1835)
oma-2(*tn1764*)	300 ± 45 (*n* = 6)	2.1 (*n* = 1797)
oma-2(*tn1764*) *lon-3*(*e2175*) *sel-10*(*ar41*)	288 ± 26 (*n* = 6)	1.1 (*n* = 1727)
oma-1(*zu405te33*)	261 ± 18 (*n* = 6)	0.8 (*n* = 1568)
oma-1(*zu405te33*); *oma-2*(*te51*) M+Z–[b]	0 (*n* > 21)[c]	NA
oma-1(*zu405te33*); *oma-2*(*cp145*)	212 ± 29 (*n* = 12)	12.3[d] (*n* = 2516)
oma-1(*zu405te33*); *oma-2*(*tn1760*)	224 ± 35 (*n* = 6)	60.3 (*n* = 1341)
oma-1(*zu405te33*); *oma-2*(*tn1764*) M+Z–[b,e]	249 ± 29 (*n* = 5)	100 (*n* > 1256)
oma-1(*zu405te33*); *oma-2*(*tn1764*) *lon-3*(*e2175*) *sel-10*(*ar41*) M+Z–[b,f]	246 ± 32 (*n* = 6)	89.4 (*n* = 1476)
oma-1(*zu405te33*); *oma-2*(*tn1764*) *lon-3*(*e2175*) *sel-10*(*ar41*)	196 ± 56 (*n* = 6)	84.9 (*n* = 1175)

[a] Average number of embryos laid per worm ± SD.
[b] M+Z– animals were the progeny of *nT1*[*qIs51*] balancer-containing parents, which are heterozygous for both *oma-1* and *oma-2*. All other animals were the progeny of parents of the listed genotype.
[c] Sterile, with a defect in meiotic maturation as described by Detwiler *et al.* (2001).
[d] Percent embryo lethality was variable among the 12 parents analyzed; it ranged between 6 and 35%.
[e] These animals lay many eggs, none of which hatch (*n* = 30).
[f] These animals lay many eggs, some of which hatch (*n* = 24).

initiation of the RNAi treatment at 22°. Because our *cul-2* (*RNAi*) clone was ineffective (see *Materials and Methods*), we also examined GFP::LIN-41 in *cul-2*(*or209*ts) mutant animals at the restrictive temperature (*n* = 71). Only the *cul-1*(*RNAi*)-treated animals produced multiple young embryos with faint GFP::LIN-41 (*n* = 12), suggesting that CUL-1 may be required to eliminate GFP::LIN-41 from embryos. *rrf-1*(*pk1417*) mutants are RNAi-defective in certain somatic cells, including the somatic gonad, but are sensitive to RNAi in the germline (Sijen *et al.* 2001; Kumsta and Hansen 2012). Treatment of *rrf-1*(*pk1417*) *lin-41*(*tn1541*) hermaphrodites with *cul-1*(*RNAi*) also resulted in the failure to eliminate GFP::LIN-41 from early embryos (*n* = 54; Figure 4C). Together, these results suggest that a germline-expressed CUL-1-containing SCF E3 ubiquitin ligase may eliminate GFP::LIN-41 from early embryos.

In SCF-type E3 ligases, cullins interact with Skp1-related proteins. Twenty-one Skp1-related (*skr*) genes have been identified in *C. elegans*, and RNAi experiments suggest the closely related *skr-1* and *skr-2* genes function in the germline and early embryo (Nayak *et al.* 2002; Yamanaka *et al.* 2002; Shirayama *et al.* 2006; Fox *et al.* 2011; Mohammad *et al.* 2018). In addition, both SKR-1 and SKR-2 can interact with CUL-1 (Nayak *et al.* 2002; Yamanaka *et al.* 2002). We therefore examined whether *skr-1*(*RNAi*), which likely reduces the function of both *skr-1* and *skr-2*, would prevent the elimination of GFP::LIN-41 from early embryos. *lin-41*(*tn1541*); *skr-1*(*RNAi*) animals produced embryos with defects in the elimination of GFP::LIN-41 2 days after RNAi treatment (*n* = 26; Figure 4B). Treatment of *rrf-1*(*pk1417*) *lin-41*(*tn1541*) animals with *skr-1*(*RNAi*) also prevented the elimination of GFP::LIN-41 from early embryos (*n* = 14). In addition, the *rrf-1*(*pk1417*) *lin-41*(*tn1541*) mutants treated with *skr-1*(*RNAi*) for 2 days at 22° exhibited defects in germline morphology and embryo production that are consistent with the phenotypes previously described after *skr-1/2*(*RNAi*) (Nayak *et al.* 2002).

At least three F-box-containing substrate recognition subunits, LIN-23, PROM-1, and SEL-10, are thought to function with either SKR-1 or SKR-2 and CUL-1 in the *C. elegans* germline or early embryos (Peel *et al.* 2012; Du *et al.* 2015; Kisielnicka *et al.* 2018; Mohammad *et al.* 2018). We used RNAi to knock down the activities of *lin-23* and *sel-10* as a first step toward the analysis of candidate F-box proteins. *lin-23*(*RNAi*) had no effect on the elimination of GFP::LIN-41 from *rrf-1*(*pk1417*) *lin-41*(*tn1541*) embryos (*n* = 52; Figure S9C). Consistent with this observation, mutations designed to prevent the phosphorylation of a possible β-TrCP/LIN-23-binding site near the amino terminus of LIN-41 (amino acids 32–38) also do not prevent the elimination of GFP::LIN-41 from embryos [*lin-41*(*tn1541tn1668*); Figure S5, D and E]. However, *sel-10*(*RNAi*) did prevent the elimination of GFP::LIN-41 from *rrf-1*(*pk1417*) *lin-41*(*tn1541*) embryos (*n* = 17). Similarly, the elimination of GFP::LIN-41 from young embryos is prevented by the strong loss-of-function mutations *sel-10*(*ok1632*) and *sel-10*(*ar41*) (Figure 4, D, E, G, and I). Whereas strong loss-of-function *sel-10* mutant alleles abrogate the rapid elimination of GFP::LIN-41 that commences upon the onset of meiotic maturation, we note that the ∼twofold decline in GFP::LIN-41 levels that occurs as oocytes progress to the −1 position (Figure 1H) occurs independently of *sel-10* (Figure 4, A, D, and E). Genetic and physical interactions indicate that SEL-10 and SKR-1 function together in *C. elegans* (Killian *et al.* 2008; Kisielnicka *et al.* 2018). Because our *skr-1*(*RNAi*) experiments are likely to also target *skr-2* (Nayak *et al.* 2002), we are unable to parse out the relative roles of SKR-1 and SKR-2 at this time. Collectively, these observations suggest that a germline-expressed $SCF^{SEL\text{-}10}$ E3 ubiquitin ligase containing SKR-1/2, CUL-1, and SEL-10 is likely involved in the elimination of GFP::LIN-41 from early embryos (Figure 5E).

SEL-10 functions through LIN-41 degradation domains

LIN-41 can be detected in *sel-10*(*ok1632*) mutant but not wild-type embryos by Western blot analysis (Figure S6D),

indicating that endogenous and GFP-tagged LIN-41 behave similarly. We hypothesized that the Deg domains are likely used to target LIN-41 for degradation by $SCF^{SEL\text{-}10}$. To test this hypothesis, we examined whether the premature elimination of mNG::Deg-A, Deg-B::OMA-2, which is mediated by the LIN-41 Deg domains, is prevented in *sel-10* mutant embryos. Although mNG::Deg-A, Deg-B::OMA-2 is eliminated by the pronuclear stage in otherwise wild-type one-cell embryos, mNG::Deg-A, Deg-B::OMA-2 levels remain high in *lon-3*(*e2175*) *sel-10*(*ar41*) embryos at the same stage of embryonic development (Figure 3, F, G, J, K, and P and Figure S7, G, H, K, and L). These observations suggest that *sel-10*(*ar41*) should suppress the completely penetrant maternal-effect lethal phenotype exhibited by *oma-1*(*zu405te33*); *oma-2*(*tn1764*) mutants. Consistent with this expectation, *oma-1*(*zu405te33*); *oma-2*(*tn1764*) *lon-3*(*e2175*) *sel-10*(*ar41*) animals produce hatchlings and can be maintained as a homozygous strain (Table 2). However, *sel-10*(*ar41*) is a relatively weak suppressor of the *oma-1*(*zu405te33*); *oma-2*(*tn1764*) maternal-effect lethal mutant phenotype, since only 10–15% of the embryos produced by *oma-1*(*zu405te33*); *oma-2*(*tn1764*) *lon-3*(*e2175*) *sel-10*(*ar41*) animals hatch. This observation is consistent with the possibility described above that the LIN-41 Deg domains might perturb the TAF-4-binding function of OMA-2 in the one-cell embryo. Additionally, *sel-10*(*ar41*) mildly reduces mNG::OMA-2 accumulation in the germline, likely through effects on GLD-1 (see below).

Although the degradation of OMA-1, and presumably OMA-2, appears to be mediated by several SCF E3 ubiquitin ligases, SEL-10 has not been implicated in this process (Shirayama *et al.* 2006; Du *et al.* 2015). Indeed, mNG::OMA-2 is degraded at the expected time in *oma-2*(*cp145*) *lon-3*(*e2175*) *sel-10*(*ar41*) embryos (Figure S7, C and D). Likewise, mNG::Deg-A, Deg-B::OMA-2 levels only remain high until the end of the one-cell stage in *oma-2*(*tn1764*) *lon-3*(*e2175*) *sel-10*(*ar41*) embryos, when the degradation of OMA-2 is normally initiated (Figure S7, K and L). We conclude that SEL-10 is not required for the elimination of OMA-2 and likely functions through the LIN-41 Deg domains to promote the proteolytic degradation of LIN-41 and mNG::Deg-A, Deg-B::OMA-2 during meiosis.

SEL-10 is required for the CDK-1-dependent elimination of GFP::LIN-41

LIN-41 Deg domains contain potential Cdc4 phosphodegron sequences: Substrate recognition subunits such as SEL-10 recognize their targets by binding to short linear sequence motifs called degrons (Lucas and Ciulli 2017). LIN-41 Deg domains were therefore examined for sequences similar to the SEL-10/Fbw7/Cdc4 degron consensus sequence ΦΦ[pT/pS]PXX[pT/pS/E/D], where Φ represents a hydrophobic amino acid. This degron is commonly referred to as a Cdc4 phosphodegron or CPD; it contains two essential residues, a phosphorylated residue that is typically a phosphothreonine, immediately followed by a proline (pTP) (Nash *et al.* 2001). SEL-10 appears to be recruited to its substrates via CPD sequences (de la Cova and Greenwald 2012). Residues surrounding LIN-41 T83, which is important for the elimination of LIN-41 from embryos, are poor matches to the CPD consensus sequence (sequence FDTPPSM, mismatches are underlined; Figure S10). The best match to a high-affinity CPD appears to be around residue T340 in the LIN-41 Deg-B2 domain (sequence LATPMSS; Figure S10), which is the only candidate Fbw7-binding site identified in LIN-41 using the Eukaryotic Linear Motif database (Gouw *et al.* 2018). However, changing T340 to an alanine (T340A) [*e.g.*, *lin-41*(*tn1541tn1775*] has no effect on the elimination of GFP::LIN-41 from embryos (Figure 2C and Figure S4, K and L). Therefore, if SEL-10 binds directly to LIN-41 Deg domains it might recognize imperfect or lower-affinity degrons. We note that the SEL-10 ortholog Cdc4p utilizes multiple imperfect degrons to target the cell division protein Sic1p for degradation (Nash *et al.* 2001). Likewise, multiple weak degrons in an intrinsically disordered region of the c-Jun protein synergize to promote a high-affinity interaction with the SEL-10 ortholog Fbw7 (Csizmok *et al.* 2018). It seems plausible that SEL-10 might function similarly. Alternatively, the failure to eliminate LIN-41 from embryos could be an indirect consequence of the lack of $SCF^{SEL\text{-}10}$. To begin to address this possibility, we sought to clarify the epistatic relationships between *sel-10* and other factors involved in the elimination of GFP::LIN-41 from embryos.

SEL-10 functions downstream or in parallel to CDK-1: CDK-1 was previously shown to be required for the elimination of GFP::LIN-41 (Spike *et al.* 2014a). Likewise, *cdk-1*(*RNAi*) on *rrf-1*(*pk1417*) *lin-41*(*tn1541*) hermaphrodites prevents the elimination of GFP::LIN-41 from embryos (n = 67; Figure S9, A and B). Therefore, germline-expressed CDK-1 likely promotes the elimination of GFP::LIN-41. CDK-1 is a conserved and essential cell cycle regulator required for M phase entry and progression during both meiotic and mitotic cell divisions (Boxem *et al.* 1999). Consequently, most *cdk-1* alleles are sterile, precluding the examination of GFP::LIN-41 in *cdk-1* mutant embryos. Two temperature-sensitive alleles of *cdk-1* that produce oocytes have been described; both cause a later embryonic arrest phenotype than the one-cell meiotic arrest phenotype seen after *cdk-1*(*RNAi*) (Boxem *et al.* 1999; Shirayama *et al.* 2006). Furthermore, although both mutations alter residues in the T-loop/activation domain of CDK-1, neither *cdk-1*(ts) allele causes obvious cell cycle defects (Shirayama *et al.* 2006). We examined GFP::LIN-41 in *cdk-1*(*ne2257*ts) animals at the restrictive temperature and found that GFP::LIN-41 disappears normally from embryos (n = 57; Figure S9, E and F). Similarly, GFP::LIN-41 disappears normally in *cks-1*(*ne549*ts) mutant embryos (n = 33; Figure S9, G and H), which phenotypically resemble *cdk-1*(*ne2257*ts) embryos at the restrictive temperature (Shirayama *et al.* 2006). Thus, the subset of CDK-1 activities affected by *cdk-1*(*ne2257*ts) does not include either the elimination of GFP::LIN-41 or entry into meiotic M phase.

SEL-10/Fbw7/Cdc4p degrons are only activated after being phosphorylated by a proline-directed serine/threonine

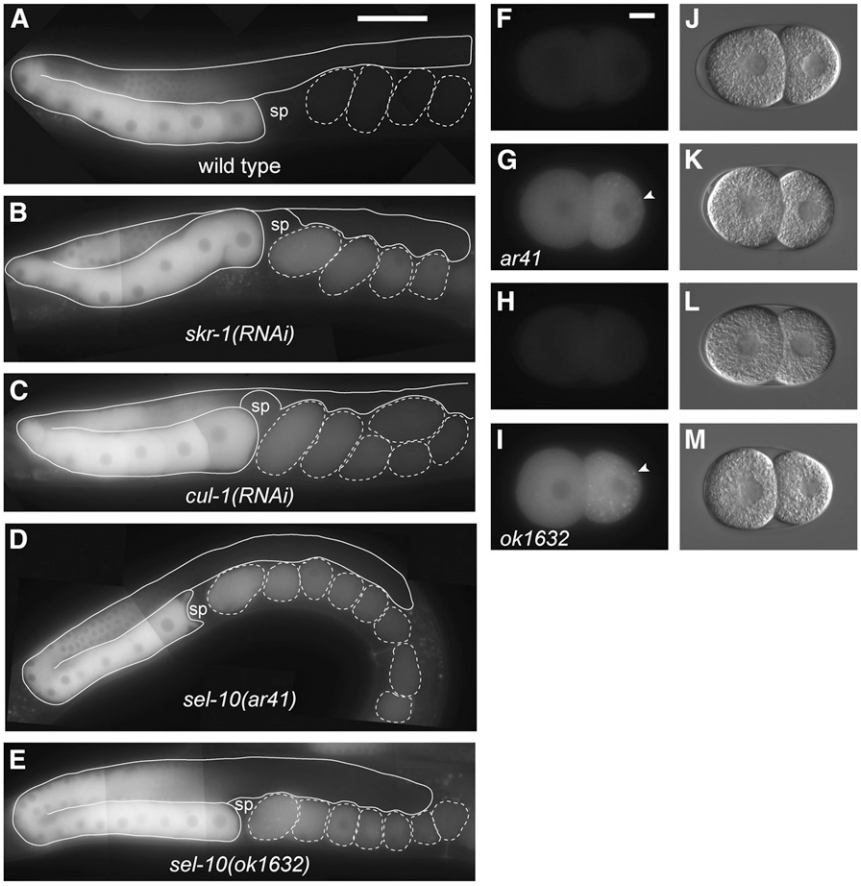

Figure 4 Subunits of the SCF^{SEL-10} E3 ubiquitin ligase are required for the elimination of GFP::LIN-41 from early embryos. (A–E) Composite images of GFP::LIN-41 in adult *rrf-1*(*pk1417*) *lin-41*(*tn1541*) hermaphrodites fed control RNAi bacteria (A), and adult hermaphrodites with reduced SCF^{SEL-10} E3 ubiquitin ligase activity (B–E): *lin-41*(*tn1541*); *skr-1* (*RNAi*) (B), *rrf-1*(*pk1417*) *lin-41*(*tn1541*); *cul-1*(*RNAi*) (C), *lin-41*(*tn1541*); *lon-3*(*e2175*) *sel-10*(*ar41*) (D), and *lin-41*(*tn1541*); *sel-10*(*ok1632*) (E); 100 ms GFP exposures, brightened slightly (and equivalently) to better visualize embryonic GFP::LIN-41; Bar, 50 μm. (F–M) Images of two-cell embryos removed from the uterus of hermaphrodites were imaged for GFP (F–I) and DIC (J–M); the genotypes were as follows: *lin-41*(*tn1541*); *lon-3*(*e2175*) (F and J), *lin-41*(*tn1541*); *lon-3*(*e2175*) *sel-10*(*ar41*) (G and K), *lin-41*(*tn1541*) (H and L), and *lin-41* (*tn1541*); *sel-10*(*ok1632*) (I and M). Arrowheads indicate a few of the GFP::LIN-41 aggregates in the posterior blastomeres of *sel-10* mutant embryos, which likely correspond to P granules; 300 ms GFP exposures; Bar, 10 μm. sp, spermatheca.

kinase such as CDK-1 (Koepp *et al.* 2001; Nash *et al.* 2001; Strohmaier *et al.* 2001; Welcker and Clurman 2008). Thus, prior phosphorylation by CDK-1 might be required for SEL-10 to directly interact with degrons in the LIN-41 Deg domains. *cdk-1*(*RNAi*) and *sel-10*(*lf*) cause the same phenotype with respect to GFP::LIN-41 degradation, precluding a direct analysis of their epistatic relationship. However, it is possible to examine this relationship indirectly through *wee-1.3* (Burrows *et al.* 2006). GFP::LIN-41 is eliminated prematurely when *wee-1.3* function is attenuated by RNAi (n = 21; Figure 5, A and B; Spike *et al.* 2014a). When the same experiment is performed in *lon-3*(*e2175*) *sel-10*(*ar41*) mutants, however, GFP::LIN-41 is not eliminated prematurely. Instead, GFP::LIN-41 persists, typically at reduced levels, in the proximal oocytes of *lon-3*(*e2175*) *sel-10*(*ar41*); *wee-1.3*(*RNAi*) animals (n = 51; Figure 5, C and D). Because CDK-1 is prematurely activated, *wee-1.3*(*RNAi*) oocytes mature prematurely and exhibit numerous defects (Burrows *et al.* 2006). Obvious oocyte abnormalities caused by strong *wee-1.3*(*RNAi*) are evident in *sel-10*(*ar41*) mutants, confirming that these animals are competent to respond to *wee-1.3*(*RNAi*) (Figure 5, compare B and D). We conclude that the epistatic relationship between *wee-1.3* and *sel-10* is consistent with the model shown in Figure 5E, which postulates that active CDK-1 promotes the phosphorylation of LIN-41 and its subsequent destruction by an SCF^{SEL-10} E3 ubiquitin ligase.

MPK-1 MAP kinase is dispensable for LIN-41 degradation: Kinases other than CDK-1 might play a role in the SEL-10-mediated elimination of LIN-41. However, our attempts to identify additional kinases that affect the elimination of GFP::LIN-41 have so far been unsuccessful. For example, the MAP kinase MPK-1 is active in the late stages of oogenesis and is an important regulator of oocyte meiotic maturation (Lee *et al.* 2007). Furthermore, as a proline-directed serine/threonine kinase, MPK-1 could potentially phosphorylate CPDs in LIN-41 Deg domains. However, GFP::LIN-41 disappears normally in *mpk-1*(*ga111*ts) embryos at the restrictive temperature (n = 97; Figure S9, I–L). We found no evidence that GFP::LIN-41 degradation involves the AIR-2/Aurora B kinase, GSK-3/glycogen synthase kinase, CDK-2, PLK-1/polo-like kinase, or MBK-2/minibrain kinase (Figure S9; Spike *et al.* 2014a). Since LIN-41 functions to inhibit CDK-1 activation for M phase entry during meiotic maturation (Spike *et al.* 2014a), CDK-1 may be the chief effector kinase mediating feedback regulation of wild-type LIN-41.

Embryonic LIN-41 does not strongly inhibit the expression of mRNAs repressed by LIN-41

LIN-41 represses the translation of several different mRNAs during oogenesis (Spike *et al.* 2014b; Tsukamoto *et al.* 2017). Their protein products normally begin to accumulate in late oogenesis or early embryogenesis, and some are essential

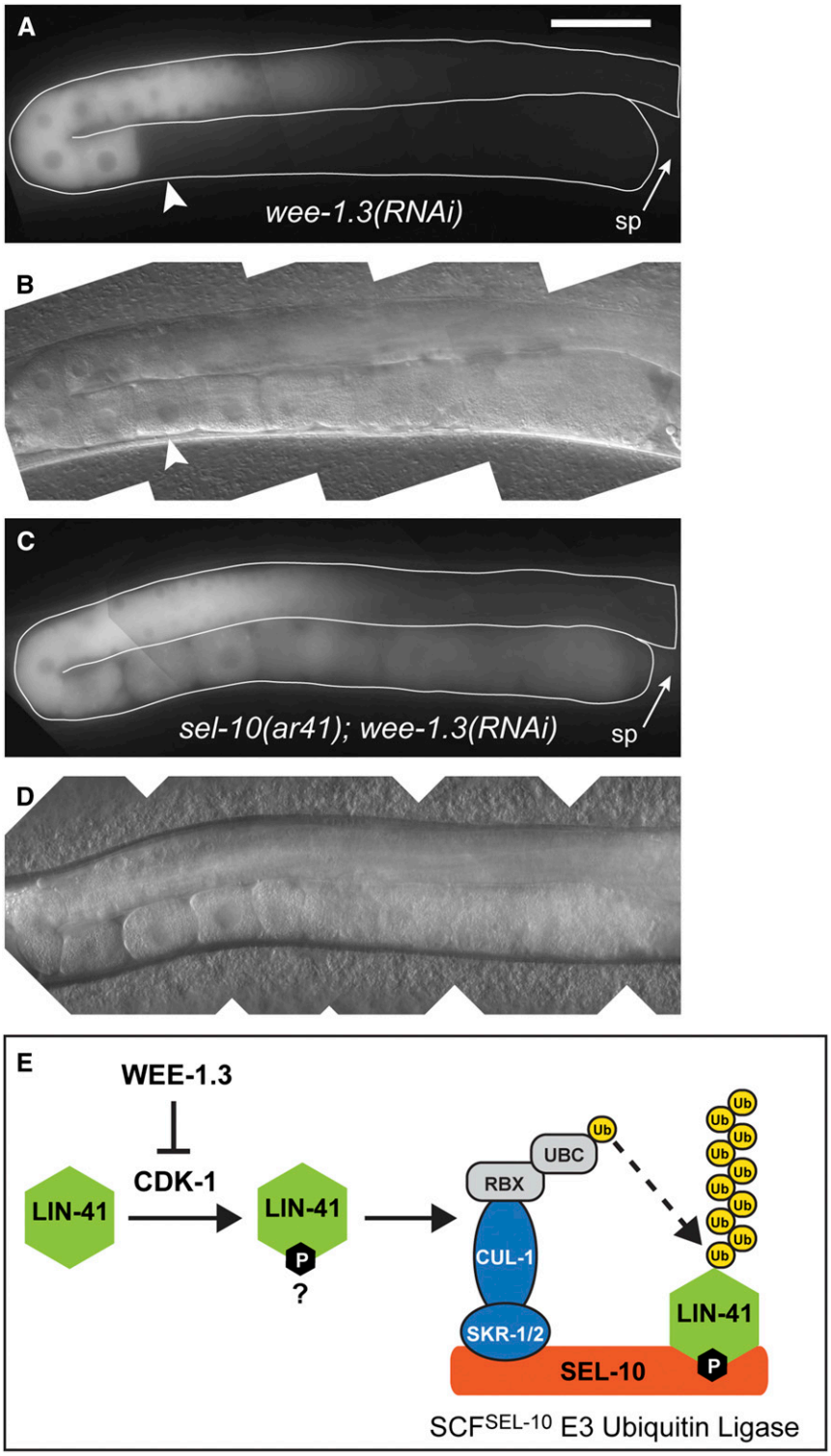

Figure 5 SEL-10 is required for the WEE-1.3–inhibited degradation of GFP::LIN-41. (A–D) Composite GFP (A and C) and DIC (B and D) images of *lin-41*(*tn1541*); *lon-3*(*e2175*); *wee-1.3*(*RNAi*) (A and B) and *lin-41*(*tn1541*); *lon-3*(*e2175*) *sel-10*(*ar41*); *wee-1.3*(*RNAi*) (C and D) animals. GFP::LIN-41 is prematurely eliminated from oocytes by *wee-1.3*(*RNAi*) (arrowhead), but persists in abnormal oocytes near the spermatheca (sp; arrow) in *sel-10* (*ar41*); *wee-1.3*(*RNAi*) animals (C and D), suggesting that SEL-10 is required for this process; 150 ms GFP exposures, brightened slightly; Bar, 50 μm. (E) A simple model for the elimination of LIN-41 (green) that incorporates the known molecular functions of WEE-1.3 kinase, cyclin-dependent kinase (CDK-1) and subunits of the SCF^{SEL-10} E3 ubiquitin ligase. In brief, we hypothesize that SEL-10 (orange) may recognize phosphorylated LIN-41 (green) and trigger its ubiquitin-mediated degradation in collaboration with the other SCF E3 ubiquitin ligase subunits, SKR-1/2 (blue), and CUL-1 (blue). CUL-1 orthologs bind RING finger proteins (RBX; gray), which recruit a ubiquitin-conjugating enzyme (UBC; gray) that catalyzes the transfer of ubiquitin (yellow) to protein substrates, such as LIN-41. Subsequent recruitment of polyubiquitinated substrates to the proteasome results in degradation (not shown). This model is consistent with the epistatic relationship between *wee-1.3*(*RNAi*) and *sel-10*(*ar41*) with respect to the elimination of GFP::LIN-41, but other models are also possible.

for normal development (Gomes *et al.* 2001; Leacock and Reinke 2008; Tsukamoto *et al.* 2017). We therefore anticipated that the failure to eliminate LIN-41 would result in the ectopic repression of these mRNAs, and that this, in turn, might result in embryo or oocyte abnormalities. However, the *lin-41*(*tn1767*) mutant, which fails to eliminate LIN-41[T83A] from early embryos, appears essentially wild type at 20° (Table 1). Similarly, *sel-10*(*ok1632*) and *sel-10*(*ar41*) mutants, which fail to eliminate LIN-41 from early embryos, produce large broods of progeny at 20° that are similar in size to genotype-matched controls (Table 3). Indeed, we only observed a moderate decrease in fertility when *sel-10*(*ok1632*) mutants were grown at an elevated temperature (25°; Table 3). We therefore decided to examine the

Table 3 *sel-10* mutant brood sizes at 20 and 25°

Genotype	Temperature	Brood size
Wild type	20	304.0 ± 31.1 (*n* = 29)
Wild type[a]	25	266.8 ± 39.0 (*n* = 19)
sel-10(*ok1632*)[a]	20	258.3 ± 67.7 (*n* = 30)
sel-10(*ok1632*)[a]	25	72.2 ± 34.0[b] (*n* = 30)
lin-41(*tn1487*ts); *sel-10*(*ok1632*)[c]	20	3.2 ± 3.4 (*n* = 53)
lin-41(*tn1487*ts)[d]	20	41.4 ± 23.8 (*n* = 36)
lon-3(*e2175*)	20	294.5 ± 36.7 (*n* = 20)
lon-3(*e2175*) *sel-10*(*ar41*)	20	280.2 ± 40.1 (*n* = 20)

[a] Newly fertilized embryos were collected at 15° and shifted to 25°.
[b] Approximately 10.0 ± 5.3% of *sel-10*(*ok1632*) hermaphrodites (*n* = 3568) are infertile, exhibiting incompletely penetrant sterility or maternal-effect lethality when grown and examined for seven generations at 25°.
[c] The progeny of *sel-10*(*ok1632*); *lin-41*(*tn1487*ts)/*hT2*[*qIs48*] hermaphrodites.
[d] The progeny of *lin-41*(*tn1487*ts)/*hT2*(*qIs48*) hermaphrodites.

amount of protein made by several LIN-41 target mRNAs (*spn-4*, *meg-1*, and *orc-1* mRNAs, respectively) in strains that fail to eliminate LIN-41 from embryos, as this should provide a sensitive way to monitor LIN-41 translational repression activity. Protein expression was examined using fluorescence-tagged alleles of each gene; the proteins made by *spn-4*(*tn1699*[*spn-4*::*gfp*::*3xflag*]), *meg-1*(*tn1724*[*gfp*::*3xflag*::*meg-1*]), and *orc-1*(*tn1732*[*mng*::*3xflag*::*orc-1*) were previously shown to be ectopically or prematurely expressed in *lin-41*(*lf*) oocytes (Tsukamoto *et al.* 2017). As described below, only minor differences in protein expression were observed in *lin-41*(*tn1767*) and *sel-10*(*ar41*) embryos and oocytes (Figure 6 and Figure S11). Collectively, these observations suggest that the ectopic LIN-41 present in *lin-41*(*tn1767*) and *sel-10*(*lf*) embryos is largely ineffective at repressing translation.

LIN-41 mediates 3′-UTR-dependent translational repression of *spn-4*, and *spn-4* mRNA is the most abundant and enriched mRNA in LIN-41 RNPs (Tsukamoto *et al.* 2017). SPN-4::GFP is faint, but visible, in one or two proximal oocytes and rapidly accumulates during the OET (Tsukamoto *et al.* 2017). This pattern, and the amount of SPN-4::GFP in early embryos, is largely unaffected by *lin-41*(*tn1767*) and *sel-10*(*ar41*) at 20° (Figure 6, A, B, G, and H, and Figure S11, A, B, K, and L). Quantification of GFP fluorescence levels revealed no differences in SPN-4::GFP levels in *lin-41*(*tn1767*); *spn-4*(*tn1699*) one- and two-cell embryos and a slight reduction in SPN-4::GFP levels in *spn-4*(*tn1699*) *lon-3*(*e2175*) *sel-10*(*ar41*) two-cell embryos relative to age and genotype-matched controls (Figure 6, K and L). Finally, we also failed to identify any apparent differences in SPN-4::GFP accumulation or intensity in *spn-4*(*tn1699*) *lon-3*(*e2175*) *sel-10*(*ar41*) (*n* = 26) and *spn-4*(*tn1699*) *lon-3*(*e2175*) (*n* = 19) animals upshifted as L4 larvae to 25°.

GFP::MEG-1 expression is evident somewhat earlier in oogenesis than SPN-4::GFP and seems to accumulate more slowly. Again, the pattern and amount of GFP::MEG-1 was largely unaffected in *lin-41*(*tn1767*) and *sel-10*(*ar41*) mutants at 20° (Figure 6, C, D, I, and J, and Figure S11, C, D, G, and H). GFP::MEG-1 has a complex pattern of accumulation in the early embryo; it appears to be eliminated from somatic blastomeres and localizes, at least partially, to P granules (Figure 6C and Figure S11C), similar to what was previously described by Leacock and Reinke (2008) for endogenous MEG-1. Because of these complexities, we quantified GFP::MEG-1 levels in the cytoplasm of proximal oocytes instead of embryos. There were no differences in GFP::MEG-1 levels in *lin-41*(*tn1767*); *meg-1*(*tn1724*) animals and only a slight reduction in the −1 oocytes of *lon-3*(*e2175*) *sel-10*(*ar41*); *meg-1*(*tn1724*) animals relative to controls. Finally, we examined *lon-3*(*e2175*) *sel-10*(*ar41*); *meg-1*(*tn1724*) (*n* = 17) and *lon-3*(*e2175*); *meg-1*(*tn1724*) (*n* = 15) animals upshifted as L4 larvae to 25°, but again failed to identify any apparent differences in GFP::MEG-1 accumulation.

mNG::ORC-1 is not visibly expressed in oocytes but becomes increasingly evident in embryos as they develop (Tsukamoto *et al.* 2017). mNG::ORC-1 associates with chromatin at certain stages of the cell cycle (Sonneville *et al.* 2012), and is faintly visible in one-cell embryos during metaphase of the first mitotic division (Figure 6E). mNG::ORC-1 was only examined in *lin-41*(*tn1767*) mutants at 20°. As for SPN-4::GFP and GFP::MEG-1, the pattern and amount of mNG::ORC-1 was largely unaffected by *lin-41*(*tn1767*) (Figure 6, E and F and Figure S11, E and F). Most importantly, the small amount of mNG::ORC-1 visible in one-cell embryos was not obviously reduced in the *lin-41*(*tn1767*) background. Because LIN-41 is a potent translational repressor of *spn-4*, *meg-1*, and *orc-1* (Tsukamoto *et al.* 2017), we conclude that a mechanism distinct from $SCF^{SEL\text{-}10}$-mediated degradation antagonizes LIN-41 function to promote their expression during the late stages of oogenesis and the OET.

Because molecular tests failed to reveal an increase in LIN-41 activity in *sel-10* mutants, we also tested the ability of a *sel-10*(*ok1632*) strong loss-of-function mutation to suppress the temperature-sensitive *lin-41*(*tn1487*ts) allele at a semipermissive temperature. This was found not to be the case; rather, *sel-10*(*ok1632*) enhanced the *lin-41*(*tn1487*ts) defects (Table 3). The basis for this enhancement is presently not clear. Taken together, these results indicate that the regulation of LIN-41 by *sel-10* is nonessential.

SEL-10 promotes the elimination of GLD-1 from oocytes

GLD-1 is a translational repressor that, like LIN-41, controls and coordinates oocyte differentiation and cell cycle progression (Francis *et al.* 1995a,b; Jones *et al.* 1996). In *gld-1*(*q485*) null mutants, pachytene-stage oocytes re-enter the mitotic cell cycle and form a tumor (Francis *et al.* 1995a,b). GLD-1 also has redundant functions to inhibit the proliferative fate of germline progenitor cells and to promote their entry into the meiotic pathway of development during oogenesis and spermatogenesis, as well as a function to promote spermatogenesis in hermaphrodites (Francis *et al.* 1995a,b; Kadyk and Kimble 1998). GLD-1 is abundantly expressed during the early and middle stages of meiotic prophase, but eliminated from oocytes as they progress from late pachytene through

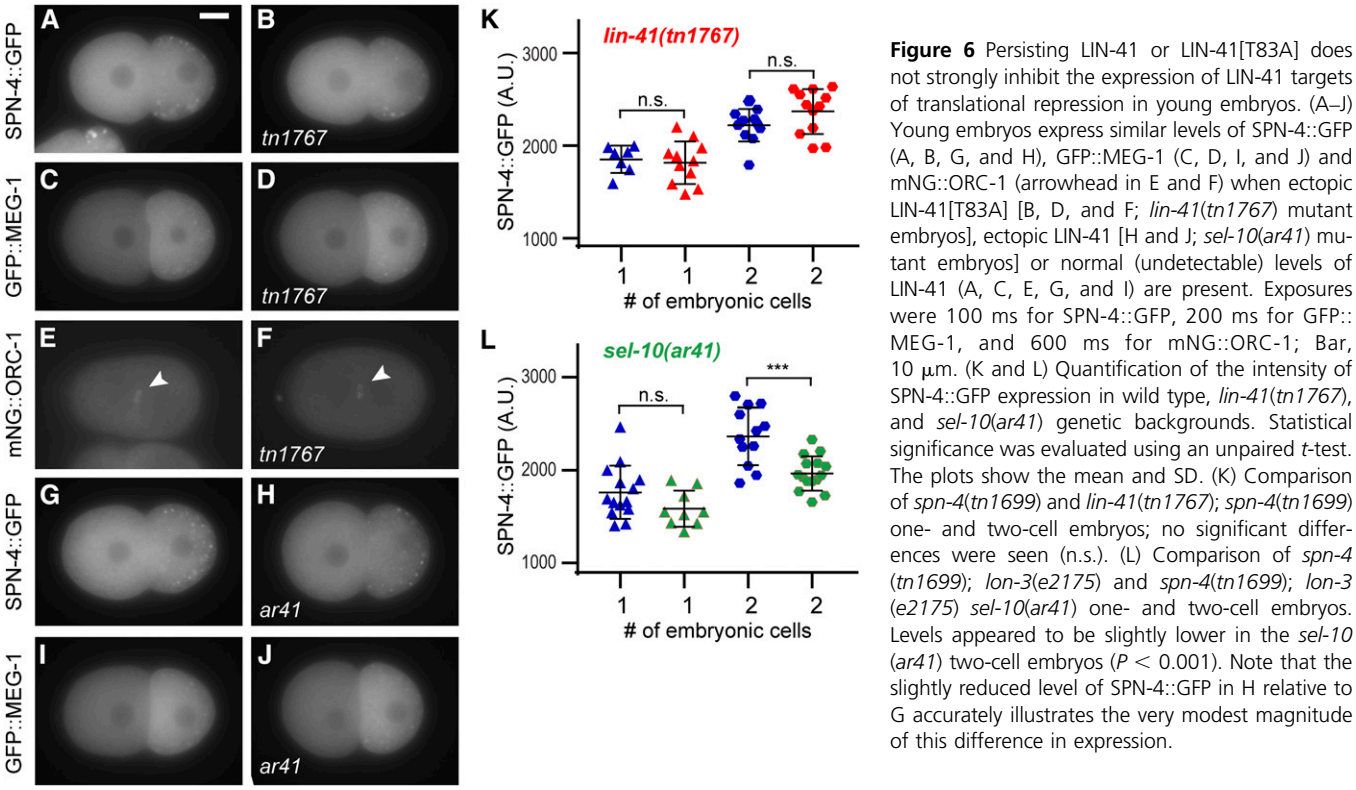

Figure 6 Persisting LIN-41 or LIN-41[T83A] does not strongly inhibit the expression of LIN-41 targets of translational repression in young embryos. (A–J) Young embryos express similar levels of SPN-4::GFP (A, B, G, and H), GFP::MEG-1 (C, D, I, and J) and mNG::ORC-1 (arrowhead in E and F) when ectopic LIN-41[T83A] [B, D, and F; *lin-41*(*tn1767*) mutant embryos], ectopic LIN-41 [H and J; *sel-10*(*ar41*) mutant embryos] or normal (undetectable) levels of LIN-41 (A, C, E, G, and I) are present. Exposures were 100 ms for SPN-4::GFP, 200 ms for GFP::MEG-1, and 600 ms for mNG::ORC-1; Bar, 10 μm. (K and L) Quantification of the intensity of SPN-4::GFP expression in wild type, *lin-41*(*tn1767*), and *sel-10*(*ar41*) genetic backgrounds. Statistical significance was evaluated using an unpaired *t*-test. The plots show the mean and SD. (K) Comparison of *spn-4*(*tn1699*) and *lin-41*(*tn1767*); *spn-4*(*tn1699*) one- and two-cell embryos; no significant differences were seen (n.s.). (L) Comparison of *spn-4* (*tn1699*); *lon-3*(*e2175*) and *spn-4*(*tn1699*); *lon-3* (*e2175*) *sel-10*(*ar41*) one- and two-cell embryos. Levels appeared to be slightly lower in the *sel-10* (*ar41*) two-cell embryos ($P < 0.001$). Note that the slightly reduced level of SPN-4::GFP in H relative to G accurately illustrates the very modest magnitude of this difference in expression.

diplotene and to diakinesis during the later stages of oocyte development (Jones *et al.* 1996). GLD-1 binds to, and represses the translation of, many mRNAs that are normally translated in oocytes (Lee and Schedl 2001, 2004; Schumacher *et al.* 2005; Jungkamp *et al.* 2011; Wright *et al.* 2011; Scheckel *et al.* 2012). Thus, it has generally been assumed that the elimination of GLD-1 from oocytes permits the translation of these mRNAs [reviewed in Lee and Schedl (2010)]. Although it occurs at an earlier stage of oocyte development, this model is analogous to what we originally hypothesized with respect to LIN-41. However, because the LIN-41 ectopically found in *sel-10* loss-of-function embryos appears to be insufficient to sustain translational repression, it seems likely that the activity of LIN-41 is also regulated by a nonproteolytic mechanism. Given the similarities between LIN-41 and GLD-1, we wondered whether GLD-1 might also be regulated by both proteolytic and nonproteolytic mechanisms.

We investigated whether the elimination of GLD-1, like LIN-41, requires SEL-10. Surprisingly, we found that GLD-1::GFP and GLD-1 do indeed persist at elevated levels in the oocytes of *sel-10*(*ar41*) and *sel-10*(*ok1632*) mutants (Figure 7, A and B and Figure S12, A, B, D, and E), indicating that LIN-41 and GLD-1 may be regulated similarly. Indeed, while we were completing this work, the failure to eliminate GLD-1 in a timely fashion from *sel-10*(*ok1632*) mutant oocytes was independently discovered by Kisielnicka *et al.* (2018). Their results suggest that both GLD-1 and the cytoplasmic polyadenylation element-binding protein CPB-3 are likely degraded by essentially the same $SCF^{SEL\text{-}10}$ E3 ubiquitin ligase (Kisielnicka *et al.* 2018) that regulates LIN-41 (this work). Consistent with this hypothesis, they observed that slow-migrating isoforms of GLD-1, which are likely phosphorylated (Jeong *et al.* 2011), accumulate in *sel-10*(*ok1632*) mutants. In agreement with this finding, we also observe an increase in the slow-migrating isoforms of GLD-1 in both *sel-10*(*ok1632*) and *sel-10*(*ar41*) mutants relative to controls (Figure 7C).

It was recently proposed that sperm trigger the proteasome-dependent elimination of GLD-1 from oocytes such that a GFP::GLD-1 transgene (an N-terminal fusion) was expressed at higher levels in unmated females than in mated females or hermaphrodites (Bohnert and Kenyon 2017). Therefore we examined the localization of a rescuing GLD-1::GFP transgene (a C-terminal fusion) in both wild-type and *sel-10*(*ar41*) mutant females, which lack sperm. We used strong loss-of-function mutations in both *fog-2* (Schedl and Kimble 1988) and *fog-3* (Ellis and Kimble 1995) to feminize the germline. However, in our experiments, GLD-1::GFP did not persist at elevated levels in female oocytes; instead, it was eliminated from oocytes in both the presence and absence of sperm (Figure 7, A and D, and Figure S12, A and C). Likewise, endogenous GLD-1, detected with specific antibodies (Jan *et al.* 1999), also disappeared from oocytes in both hermaphrodites and females (Figure S12, D and F). However, GLD-1::GFP levels remained elevated in the oocytes of *sel-10*(*ar41*) mutant females (Figure 7E). Oocytes remain in the gonad for an extended period of time in the absence of sperm (McCarter *et al.* 1999). Indeed, we noticed that there seemed to be relatively less GLD-1::GFP in the *sel-*

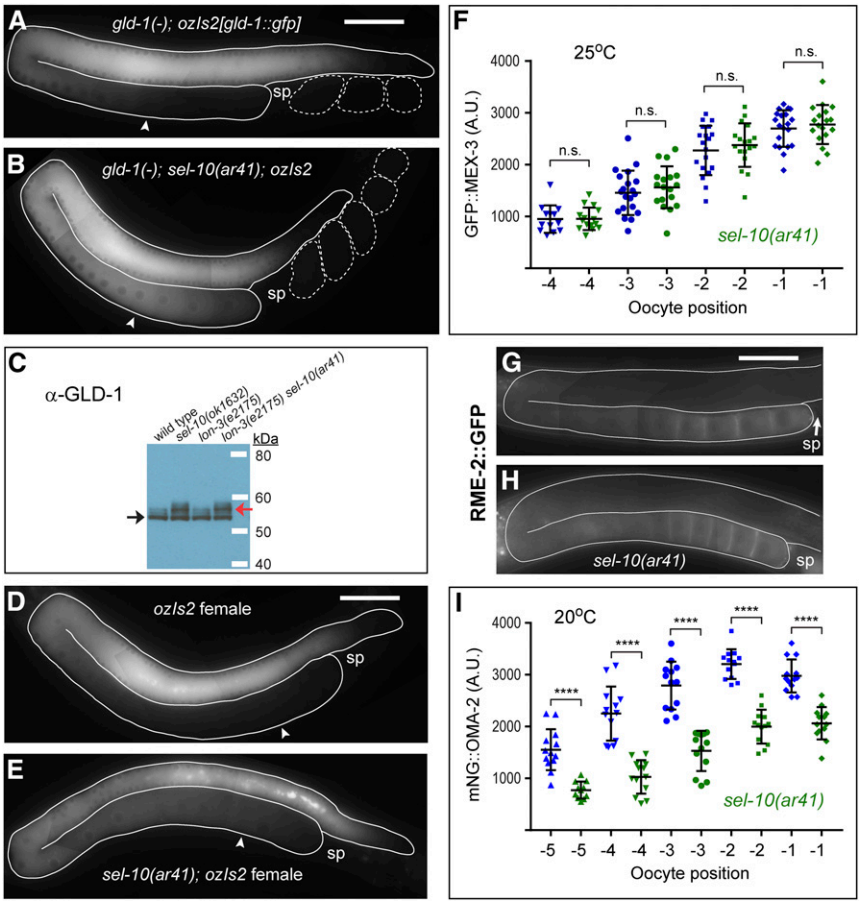

Figure 7 GLD-1 persists at elevated levels in the oocytes of *sel-10*(*ar41*) mutants. (A and B) Composite images of GLD-1::GFP in *gld-1*(*q485*); *lon-3* (*e2175*); *ozIs2*[*gld-1*::*gfp*] (A) and *gld-1*(*q485*); *lon-3*(*e2175*) *sel-10*(*ar41*); *ozIs2*[*gld-1*::*gfp*] (B) adult hermaphrodites. GLD-1::GFP levels remain elevated in the proximal oocytes (*e.g.*, −4 oocytes, arrowheads) of *sel-10*(*ar41*) animals (B) relative to controls (A); 17 ms GFP exposures, brightened slightly. (C) Slow-migrating forms of GLD-1 (red arrow) are more abundant in *sel-10*(*lf*) adult hermaphrodites than in *sel-10*(+) controls, where the fast-migrating form of GLD-1 (black arrow) predominates. (D and E) Composite images of GLD-1::GFP in *fog-3*(*q470*); *lon-3*(*e2175*); *ozIs2*[*gld-1*::*gfp*] (D) and *fog-3*(*q470*); *lon-3*(*e2175*) *sel-10*(*ar41*); *ozIs2*[*gld-1*::*gfp*] females (E). GLD-1::GFP levels are elevated in the proximal oocytes (*e.g.*, −4 oocytes, arrowheads) of *sel-10* (*ar41*) females (B) relative to controls (A), although this is not as dramatic as in hermaphrodites. A somewhat longer GFP exposure (35 ms, brightened slightly) was needed than in A and B, likely due to the presence of endogenous GLD-1. (F) Quantification of the intensity of GFP::MEX-3 in the proximal oocytes of *lon-3*(*e2175*); *mex-3*(*tn1753*) and *lon-3* (*e2175*) *sel-10*(*ar41*); *mex-3*(*tn1753*) hermaphrodites at 25°. No significant differences were seen (n.s.). (G and H) Composite images of *lon-3* (*e2175*); *pwIs116*[*rme-2p*::*rme-2*::*GFP*::*rme-2 3′UTR*] (G) and *lon-3*(*e2175*) *sel-10*(*ar41*); *pwIs116* [*rme-2p*::*rme-2*::*GFP*::*rme-2 3′UTR*] (H) hermaphrodites at 22°; 300 ms GFP exposures. Neither target of GLD-1 translational repression (MEX-3, RME-2) was strongly or even marginally reduced in expression in *sel-10*(*ar41*) oocytes. (I) Quantification of the intensity of mNG::OMA-2 in the proximal oocytes of *oma-2*(*cp145*) *lon-3*(*e2175*) and *oma-2*(*cp145*) *lon-3*(*e2175*) *sel-10*(*ar41*) hermaphrodites at 20°. Differences in expression were highly significant (**** $P < 0.0001$), but relatively modest in magnitude. For example, we measured a 37% reduction in average fluorescence in the −2 oocytes of *sel-10*(*ar41*) animals relative to the same oocytes in control animals. Statistical tests (F and I) employed an unpaired *t*-test. The plots show the mean and SD. All phenotypes were analyzed on the first day of adulthood. Bar, 50 μm (A, B, D, E, G, and H). sp, spermatheca.

10(*ar41*) oocytes of females as compared to hermaphrodites, possibly as a result of *sel-10*-independent protein turnover. From these results, we conclude that the *sel-10*-dependent elimination of GLD-1::GFP is sperm-independent. Furthermore, the expression patterns of GLD-1::GFP, which rescues the *gld-1*(*q485*) null mutation to fertility (Schumacher *et al.* 2005; Figure 7A), and endogenous GLD-1 (Figure S12, D and F), fail to support the hypothesis that sperm trigger the elimination of GLD-1 from oocytes. We have tested the GFP::GLD-1 transgene (*axIs1498*[*pie-1p*::*gfp*::*gld-1*::*gld-1 3′UTR*, *unc-119*(+)]; Merritt *et al.* 2008) used by Bohnert and Kenyon (2017) to monitor GLD-1 expression in females; however, we found that it fails to rescue *gld-1*(*q485*) null mutants to fertility. Adult *gld-1*(*q485*); *axIs1498* hermaphrodites are invariably sterile and exhibit a range of phenotypes from a tumorous phenotype that is equivalent to the null allele to the production of abnormal oocytes. We analyzed 192 progeny from *gld-1*(*q485*)/+; *axIs1498* adult hermaphrodites; 53 (27.6%) were *gld-1*(*q485*); *axIs1498* and were sterile, consistent with the inability of *axIs1498* to provide wild-type *gld-1* function. We conclude that the increased expression of GFP::GLD-1 observed in the oocytes of *axIs1498* females (Bohnert and Kenyon 2017) is most likely a transgene expression artifact and does not reflect the expression and regulation of endogenous GLD-1.

Ectopic GLD-1 in proximal oocytes does not strongly inhibit the expression of mRNAs repressed by GLD-1

As for LIN-41, we examined whether the mRNA targets of GLD-1-mediated translational repression are ectopically repressed in *sel-10*(*ar41*) mutant oocytes. Studies of GLD-1 function in the proliferative *vs.* meiotic entry decision of germline progenitor cells demonstrate that GLP-1/Notch signaling functions to inhibit GLD-1 accumulation in the distal end of the germline (Hansen and Schedl 2013). When GLD-1 accumulates ectopically in the distal stem cell niche in *glp-1* mutants, or double mutants affecting the Pumilio and FBF proteins FBF-1 and FBF-2, germline progenitor cells fail to proliferate and prematurely enter the meiotic pathway of development (Crittenden *et al.* 2002; Hansen *et al.* 2004). Thus, our initial expectation was that ectopic GLD-1 expression in proximal oocytes in strong *sel-10* loss-of-function mutants might exert substantial effects on the repression of its mRNA

targets. As for LIN-41, this proved not to be the case; only subtle or modest effects were observed, as described below.

GLD-1 binds the 3′-UTR of the *spn-4* mRNA (Jungkamp *et al.* 2011), which we initially examined as a LIN-41 target, and GLD-1 appears to repress SPN-4 accumulation in the distal germline (Mootz *et al.* 2004). As described previously, SPN-4::GFP expression was not strongly affected by the *sel-10*(*ar41*) mutation (Figure S11, I–L) despite the ectopic expression of both GLD-1 and LIN-41 (Figure 4 and Figure 7). MEX-3 is expressed in proximal oocytes and also appears to be repressed by GLD-1 (Mootz *et al.* 2004; Jungkamp *et al.* 2011). We used the fluorescence-tagged *mex-3*(*tn1753* [*gfp*::*3xflag*::*mex-3*]) allele to quantitatively examine the expression of GFP::MEX-3 in these oocytes at both 20 and 25°. GFP::MEX-3 levels were not reduced in *sel-10*(*ar41*) oocytes at either temperature, but were generally very similar to the wild-type controls (Figure 7F, and Figure S12H). In addition, we examined the expression of the yolk receptor RME-2 (Grant and Hirsh 1999), a well-established target of GLD-1-mediated translational repression (Lee and Schedl 2001; Jungkamp *et al.* 2011; Wright *et al.* 2011). We began by examining the expression of RME-2::GFP from *pwIs116*[*rme-2p*::*rme-2*::*GFP*::*rme-2 3′UTR*] in oocytes at 22°, to prevent transgene silencing. Again, the levels of RME-2::GFP were similar in the proximal oocytes of *sel-10*(*ar41*) and wild-type controls (Figure 7, G and H). Likewise, similar levels of endogenous RME-2 were seen in *sel-10*(*ok1632*) and wild-type oocytes stained with anti-RME-2-specific antibodies (Figure S12, I and J). Finally, we examined the expression of OMA-2, another well-established target of GLD-1-mediated translational repression (Lee and Schedl 2004; Wright *et al.* 2011; Scheckel *et al.* 2012). We quantitatively compared the expression level of mNG::OMA-2 expression in the proximal oocytes of the wild type and *sel-10*(*ar41*) mutants and observed a modest reduction (∼30–50%) in mNG::OMA-2 expression levels in *sel-10*(*ar41*) mutants (Figure 7I). This result is agreement with the finding that an antibody that detects OMA-2 and its paralog OMA-1 exhibits a modest reduction in immunofluorescence staining (∼10–33%, depending on the region of the proximal gonad analyzed) in the *sel-10*(*ok1632*) strong loss-of-function mutant (Kisielnicka *et al.* 2018).

Collectively, these results suggest that the ectopic GLD-1 in *sel-10* mutant oocytes is minimally effective at repressing translation of mRNA targets. The observation that some targets (*e.g.*, *spn-4*, *mex-3*, and *rme-2*) might be unaffected by ectopic GLD-1, whereas others (*e.g.*, *oma-2*) are modestly affected, is consistent with the observation that certain *gld-1* mutant alleles disrupt binding and repression of some mRNA targets but not others (Schumacher *et al.* 2005). Furthermore, these observations are again consistent with the fact that *sel-10* mutants are viable and fertile (Table 3), as the efficient repression of proteins such as SPN-4, MEX-3, and RME-2 during oogenesis should have negative consequences for embryonic development (Draper *et al.* 1996; Grant and Hirsh 1999; Gomes *et al.* 2001).

The SCF^{SEL-10}-dependent degradation of LIN-41 and GLD-1 depend on different kinases

As described above, the SCF^{SEL-10}-dependent degradation of LIN-41 depends on CDK-1, but not MPK-1 (Figure S9, I–L). Consequently, we examined the requirement of these kinases for the SCF^{SEL-10}-dependent degradation of GLD-1. Whereas *cdk-1*(*RNAi*) or *cdk-2*(*RNAi*) had no effect on the accumulation of GLD-1::GFP in proximal oocytes ($n = 14$ and $n = 23$, respectively), we observed ectopic expression of GLD-1::GFP in the proximal oocytes of *ozIs5*[*gld-1*::*gfp*]; *mpk-1*(*ga111*ts) hermaphrodites at the nonpermissive temperature (Figure S13). Thus, although both GLD-1 and LIN-41 are regulated by SCF^{SEL-10}-dependent degradation, the temporal and spatial control of their accumulation during oogenesis is differentially responsive to protein kinase signaling, befitting their individual biological functions in promoting oogenesis.

Discussion

Feedback regulation of LIN-41 and the spatial control of oocyte meiotic maturation

The oocytes of most sexually reproducing animals arrest in meiotic prophase for a prolonged period [reviewed by Huelgas-Morales and Greenstein (2017), Avilés-Pagán and Orr-Weaver (2018)]. This conserved arrest likely enables transcriptionally quiescent oocytes to grow by accumulating cellular organelles and cytoplasmic factors needed for embryonic development. Indeed, in *C. elegans* oocyte growth and meiotic maturation are coordinately controlled by LIN-41. In the absence of LIN-41 function, pachytene-stage oocytes abruptly cellularize, activate CDK-1, and enter M phase (Spike *et al.* 2014a). A salient feature of *C. elegans* oogenesis is that meiotic maturation is restricted to the oocyte in the most proximal position adjacent to the spermatheca. This restriction ensures that only fully grown oocytes undergo meiotic maturation when they are positioned to enter the spermatheca during ovulation so they can become fertilized. Genetic evidence suggests that OMA proteins function to inhibit LIN-41 to facilitate meiotic maturation of the most proximal oocyte (Spike *et al.* 2014a). Specifically, proximal oocytes fail to enter M phase in *lin-41*(ts); *oma-1*(*null*); *oma-2*(*null*) triple mutants; whereas pachytene stage oocytes prematurely enter M phase in *lin-41*(*null*); *oma-1*(*null*); *oma-2*(*null*) triple mutants (Spike *et al.* 2014a). Thus, the OMA proteins are absolutely required to spatially restrict M phase entry to the –1 oocyte, where they counteract the inhibitory activity of LIN-41. Consistent with this idea, molecular evidence suggests that LIN-41 is inactivated as a translational repressor in the final stages of oogenesis (Spike *et al.* 2014a; Tsukamoto *et al.* 2017), which precedes the elimination of LIN-41 upon the onset of meiotic maturation. Specifically, two targets of LIN-41-mediated translational

repression, *spn-4* and *meg-1*, are coexpressed with LIN-41 in the most proximal oocytes. The expression of *spn-4* and *meg-1* in proximal oocytes requires the function of the OMA proteins (Tsukamoto *et al.* 2017), consistent with the idea that the OMA proteins antagonize LIN-41 function in the late stages of oogenesis.

Here we show that $SCF^{SEL\text{-}10}$ promotes the rapid ubiquitin-mediated degradation of LIN-41 that leads to its elimination during meiosis I. Analysis of *sel-10* mutants indicates that the inactivation and degradation of LIN-41 are separable; the LIN-41 that accumulates in *sel-10* mutants appears to be largely inactive as a translational repressor. However, we did note that several LIN-41 variants (LIN-41[T83A] and LIN-41[ΔDeg-A]), which are defective in the $SCF^{SEL\text{-}10}$-mediated degradation, decrease the meiotic maturation rate. This finding is consistent with the idea that LIN-41 inhibits meiotic maturation and that $SCF^{SEL\text{-}10}$-mediated degradation constitutes a nonessential component of the regulatory mechanism. The nature of the "primary" mechanism inactivating LIN-41 prior to its degradation is currently unknown but could act on LIN-41 directly or another component of the large RNP complex it associates with (Spike *et al.* 2014b; Tsukamoto *et al.* 2017).

LIN-41 and CDK-1 reciprocally inhibit each other's activity. Thus, the primary inactivation mechanism might play a key role in tipping the balance between LIN-41 and CDK-1 to generate a spatially restricted all-or-none meiotic maturation response. Upon its activation, CDK-1 triggers meiotic maturation and promotes the $SCF^{SEL\text{-}10}$-dependent elimination of LIN-41. The elimination of LIN-41 requires the Deg-A and Deg-B domains in the LIN-41 N-terminal region. The LIN-41 Deg-A and Deg-B domains are intrinsically disordered and contain sequences that might function as phosphodegrons. The $SCF^{SEL\text{-}10}$-dependent elimination of LIN-41 is blocked by the T83A mutation affecting a potential CDK-1 phosphorylation site within the Deg-A domain, although whether this regulation is direct or indirect remains to be determined. We note one exception to the rule that CDK-1 activity promotes LIN-41 degradation. The *lin-41*(*tn1541-tn1618*) mutation (Figure 2), which deletes the NHL domain, produces a strong loss-of-function *lin-41* mutant phenotype in which pachytene-stage oocytes enter M phase precociously. Nonetheless, we observe that the GFP::LIN-41 (ΔNHL) protein still accumulates in the proximal gonad, albeit in an aberrantly punctate pattern (Figure S3, G–J). Interestingly, in the presence of a wild-type LIN-41 protein, the GFP::LIN-41(ΔNHL) mutant protein accumulates normally and is subject to $SCF^{SEL\text{-}10}$-dependent degradation on schedule. It may be that the accumulation of the GFP::LIN-41(ΔNHL) protein in a punctate pattern correlates with its inaccessibility to CDK-1-dependent regulation. Alternatively, the degradation of LIN-41 during meiotic maturation may depend on LIN-41 activity during pachytene, as could be the case if a component of the $SCF^{SEL\text{-}10}$ degradation mechanism depends on *lin-41* function for its synthesis or activity.

The Deg domains may function as a timer to ensure that CDK-1 activity reaches an optimal threshold to ensure the successful completion of the meiotic divisions prior to the initiation of LIN-41 degradation. If LIN-41 is eliminated too early, the fidelity of meiotic chromosome segregation may be compromised, as is observed in certain hypomorphic *lin-41* mutant alleles (*e.g.*, *tn1487tn1515*, *tn1487tn1516*, *tn1487tn1536*, and *tn1487tn1539*; Spike *et al.* 2014a). Thus, it will be important to elucidate the precise mechanisms by which the LIN-41 Deg domains link CDK-1 activity to $SCF^{SEL\text{-}10}$-mediated degradation. The regulation of the G1/S phase transition in budding yeast provides a framework for thinking about this issue [Nash *et al.* 2001; Kõivomägi *et al.* 2011; Yang *et al.* 2013; reviewed by Hopkins *et al.* (2017)]. The cyclin-dependent kinase complex, Cdk1-Clb5/6, promotes the entry into S phase but is inhibited by binding to its inhibitor Sic1 (Nugroho and Mendenhall 1994; Schwob *et al.* 1994). Sic1 is a substrate of the Cdk1-Clb5/6 kinase, which phosphorylates Sic1 to promote SCF^{Cdc4}-mediated degradation (Feldman *et al.* 1997; Verma *et al.* 1997; Nash *et al.* 2001). The cyclin-dependent kinase Cdk1-Cln1/2 initiates the decision to enter S phase during G1 and is not inhibited by Sic1. Phosphorylation of Sic1 by Cdk1-Cln1/2, while not sufficient to trigger Sic1 degradation, primes Sic1 for multisite phosphorylation by Clb5/6. The Sic1 CPD sequences contain multiple sites for phosphorylation by both Cdk1-Clb5/6 and Cdk1-Cln1/2, which results in the switch-like destruction of Sic1. A failure to degrade Sic1 substantially delays the G1/S transition, whereas deletion of SIC1 causes DNA replication to initiate too early, resulting in genome instability (Nugroho and Mendenhall 1994; Cross *et al.* 2007). Further dissection of the mechanism by which the LIN-41 Deg domains function will illuminate whether analogous mechanisms are employed in a developmental context.

Ubiquitin-mediated protein degradation and the OET

Signaling pathways and downstream kinase activation coordinate the cell cycle and developmental events that underpin oocyte and early embryo development. In *C. elegans* the ERK MAP kinase signaling pathway and its effector kinase MPK-1 regulate pachytene progression and multiple aspects of oogenesis, including oocyte growth and specific events that occur during meiotic maturation [reviewed by Arur (2017)]. Consistent with these phenotypes, sustained activation of MPK-1 occurs during pachytene and in proximal oocytes (Lee *et al.* 2007). Likewise, in proximal oocytes activated cyclin-dependent kinase CDK-1 regulates an important aspect of oocyte meiotic maturation by promoting the transition from meiotic prophase to meiotic M phase, as we have described. Once activated, CDK-1 phosphorylates the DYRK mini-brain kinase MBK-2 as part of an intricate regulatory mechanism that permits MBK-2 activation near the end of the first meiotic division (Pellettieri *et al.* 2003; Stitzel *et al.* 2006, 2007; Cheng *et al.* 2009; Parry *et al.* 2009). These three kinases (MPK-1, CDK-1, and MBK-2) all function, at least in

part, to promote the degradation of one or more RNA-binding proteins during oogenesis or the OET.

After meiosis, the OMA proteins are detectably phosphorylated by activated MBK-2 (Nishi and Lin 2005). Phosphorylation by MBK-2 promotes a direct physical interaction between the OMA proteins and the transcription factor TAF-4; this permits the sequestration of TAF-4 in the cytoplasm and prevents the premature onset of zygotic transcription (Guven-Ozkan *et al.* 2008). Furthermore, MBK-2-dependent phosphorylation primes the OMA proteins for phosphorylation by the glycogen synthase kinase GSK-3 and for degradation during the first mitotic division (Nishi and Lin 2005; Shirayama *et al.* 2006). In addition to MBK-2 and GSK-3, the degradation of the OMA proteins requires the normal activities of additional kinases, including CDK-1/Cyclin B3, and several proposed E3 ubiquitin ligases (Shirayama *et al.* 2006; Du *et al.* 2015). The failure to degrade OMA-1 and eliminate it from early embryos is deleterious (Lin 2003) and contributes to phenotypes exhibited by mutants that fail to degrade the OMA proteins (Shirayama *et al.* 2006). Indeed, the ectopic expression of OMA-1 in early embryos represses the translation of at least one mRNA target of the OMA proteins, *zif-1* mRNA, but only when OMA-1 is not phosphorylated by MBK-2, as in the *oma-1*(*zu405*gf) mutant (Guven-Ozkan *et al.* 2010). Thus, the MBK-2-dependent phosphorylation of the OMA proteins not only primes these proteins for degradation but also inhibits their ability to function as translational repressors.

Likewise, the ability of GLD-1 to function as a translational repressor might be inhibited by MPK-1-dependent phosphorylation (Kisielnicka *et al.* 2018; this work). Since *mpk-1* activity is also required for the elimination of GLD-1, MPK-1-dependent phosphorylation would coordinate the inactivation of GLD-1 as a translational repressor with GLD-1 degradation. Consistent with this hypothesis, MPK-1 promotes the phosphorylation of GLD-1 and promotes its $SCF^{SEL\text{-}10}$-mediated degradation (Kisielnicka *et al.* 2018; this work). Furthermore, this hypothesis potentially explains why the ectopic GLD-1 expressed in *sel-10* mutant oocytes is relatively ineffective at repressing the translation of multiple target mRNAs.

In sharp contrast to OMA-1 and GLD-1, our current understanding of the regulation of LIN-41 suggests that the inactivation of LIN-41 as a translational repressor is temporally and molecularly distinct from its degradation. Targets of LIN-41 translational repression such as *spn-4* and *meg-1* are actively translated prior to meiotic maturation and the CDK-1-dependent elimination of LIN-41. We have not yet determined that LIN-41 is phosphorylated by CDK-1 or any other kinase, as electrophoretic mobility changes are not reproducibly observed in *sel-10* mutants using several standard gel systems (Figure S6D and C. Spike and D. Greenstein, unpublished results). Using the Phos-Tag gel system, which is useful for detecting phosphoproteins (Wang *et al.* 2014), the total LIN-41 from *sel-10* mutant adults migrates more slowly; however, we are uncertain as to whether this is due to phosphorylation (C. Spike and D. Greenstein, unpublished results). The fact that *spn-4* and *meg-1* mRNAs are translated normally when *cdk-1* function is attenuated by RNAi (Tsukamoto *et al.* 2017) suggests that the CDK-1 is not required to inactivate LIN-41 as a translational repressor. In addition, we show here that mutations affecting the function of the LIN-41 Deg domains do not exhibit gain-of-function phenotypes or substantially repress the translation of LIN-41 target mRNAs.

Multiple mechanisms regulate LIN-41 proteins

LIN-41 was first identified through its role in the heterochronic gene regulatory pathway that controls the timing of postembryonic cell divisions and cell fate decisions in somatic cells in *C. elegans* [Reinhart *et al.* 2000; Slack *et al.* 2000; reviewed by Rougvie and Moss (2013)]. In this capacity, LIN-41 functions to repress the translation of several transcription factors, including LIN-29, MAB-3, MAB-10, and DMD-3, which play key roles in specifying somatic cell fates during the L4 and adult stages (Reinhart *et al.* 2000; Harris and Horvitz 2011; Aeschimann *et al.* 2017). LIN-41 binds to the mRNAs of these genes and represses their translation during early larval stages (*e.g.*, L1–L3) (Aeschimann *et al.* 2017). The *let-7* microRNA promotes the switch from early larval stages to the L4 and adult stages by repressing translation of LIN-41 beginning in the L4 stage (Reinhart *et al.* 2000; Slack *et al.* 2000). This regulation is specific to the soma as the *let-7*(*n2583*ts) mutation does not increase the accumulation of LIN-41 in the oogenic germline (Spike *et al.* 2014a). It is not clear whether specific protein degradation mechanisms collaborate with Let-7-mediated regulation to ensure that LIN-41 does not perdure from the early larval stages into the L4 and adult stage in somatic cells. If such mechanisms exist, they are unlikely to depend solely on the Deg domains because *lin-41* mutations affecting the Deg domains (*e.g.*, *tn1620*, *tn1622 tn1635*, *tn1638*, *tn1643*, and *tn1645*) do not phenocopy *let-7* mutations or exhibit dominant somatic defects. Additionally, the Deg mutations do not confer an overt *lin-41*(*lf*) Dpy phenotype. Further, *lin-41*(*tn1541tn1643*[*ΔDeg-A–RING–Deg-B*]) L3-stage larvae do not exhibit precocious adult alae ($n = 7$; Ann Rougvie, personal communication) as is frequently observed in *lin-41*(*lf*) mutants (Slack *et al.* 2000). The Deg domains mediate LIN-41 degradation during the OET over short timescales (*i.e.*, 10–15 min), whereas the larval stages last for hours. This difference may obviate a requirement for $SCF^{SEL\text{-}10}$-mediated degradation of LIN-41 during the larval stages. Interestingly, several *lin-41* gain-of-function alleles affecting the N-terminal 39 amino acid residues result in a defect in tip retraction during male tail development resulting in the production of a leptoderan (Lep) tail characteristic of other rhabditid nematode species (Del Rio-Albrechtsen *et al.* 2006). These *lin-41*(*Lep*) gain-of-function alleles do not affect LIN-41 degradation during the OET and thus define a site for LIN-41 regulation in somatic cells, which could involve proteolytic degradation.

LIN-41 is highly conserved. The mammalian ortholog LIN-41/TRIM71 is required for embryonic viability and neural

tube closure in mice (Maller Schulman *et al.* 2008; Cuevas *et al.* 2015; Mitschka *et al.* 2015). LIN-41/TRIM71 was found to promote reprogramming of dermal fibroblasts to induced-pluripotent stem cells through the negative regulation of differentiation genes, including the transcription factor EGR1 (Worringer *et al.* 2014). Importantly, the *let-7* microRNA inhibits reprogramming in part through the repression of LIN-41. Thus, the regulation of LIN-41 by Let-7 is a conserved regulatory module. By contrast, the Deg domains of *C. elegans* LIN-41 are not conserved at the amino acid sequence level in the mammalian orthologs and appear to be rapidly evolving in closely related rhabditid nematodes.

Developing systems must deploy mechanisms to extinguish translational repression mediated by RNA-binding proteins. Such mechanisms may function to promote translation of batteries of genes needed to drive developmental transitions. LIN-41-associated mRNAs include many key genes required for embryonic development (Tsukamoto *et al.* 2017). Thus, inactivation of LIN-41 likely plays a key role in shaping the proteome during the OET. The primary mechanism inactivating LIN-41 prior to its degradation, and its potential conservation in LIN-41 orthologs or members of the TRIM-NHL class of RNA-binding proteins, remain to be determined.

Acknowledgments

We are grateful to Swathi Arur, Sarah Crittenden, Claire de la Cova, Daniel Dickinson, Bob Goldstein, Barth Grant, Iva Greenwald, Judith Kimble, Tim Schedl, and Dustin Updike for providing strains or reagents. We thank G. W. Gant Luxton for the use of his spinning disc confocal microscope. We also thank WormBase for sequences and annotations. We thank Cynthia Kenyon for discussions on GLD-1 regulation. Ann Rougvie and Todd Starich provided helpful suggestions during the course of this work. Some strains were provided by the *Caenorhabditis* Genetics Center, which is funded by grant P40OD010440 from the National Institutes of Health Office of Research Infrastructure Programs. This work was supported by National Institutes of Health grant GM57173 (to D.G.).

Literature Cited

Aeschimann, F., P. Kumari, H. Bartake, D. Gaidatzis, L. Xu *et al.*, 2017 LIN41 post-transcriptionally silences mRNAs by two distinct and position-dependent mechanisms. Mol. Cell 65: 476–489.e4. https://doi.org/10.1016/j.molcel.2016.12.010

Allen, A. K., J. E. Nesmith, and A. Golden, 2014 An RNAi-based suppressor screen identifies interactors of the Myt1 ortholog *of Caenorhabditis elegans*. G3 (Bethesda) 4: 2329–2343. https://doi.org/10.1534/g3.114.013649

Arribere, J. A., R. T. Bell, B. X. Fu, K. L. Artiles, P. S. Hartman *et al.*, 2014 Efficient marker-free recovery of custom genetic modifications with CRISPR/Cas9 in *Caenorhabditis elegans*. Genetics 198: 837–846. https://doi.org/10.1534/genetics.114.169730

Arur, S., 2017 Signaling-mediated regulation of meiotic prophase I and transition during oogenesis. Results Probl. Cell Differ. 59: 101–123. https://doi.org/10.1007/978-3-319-44820-6_4

Avilés-Pagán, E. E., and T. L. Orr-Weaver, 2018 Activating embryonic development in *Drosophila*. Semin. Cell Dev. Biol. (in press). https://doi.org/10.1016/j.semcdb.2018.02.019

Balklava, Z., S. Pant, H. Fares, and B. D. Grant, 2007 Genome-wide analysis identifies a general requirement for polarity proteins in endocytic traffic. Nat. Cell Biol. 9: 1066–1073. https://doi.org/10.1038/ncb1627

Beard, S. M., R. B. Smit, B. G. Chan, and P. E. Mains, 2016 Regulation of the MEI-1/MEI-2 microtubule-severing Katanin complex in early *Caenorhabditis elegans* development. G3 (Bethesda) 6: 3257–3268.

Boag, P. R., A. Nakamura, and T. K. Blackwell, 2005 A conserved RNA-protein complex component involved in physiological germline apoptosis regulation in *C. elegans*. Development 132: 4975–4986. https://doi.org/10.1242/dev.02060

Bohnert, K. A., and C. Kenyon, 2017 A lysosomal switch triggers proteostasis renewal in the immortal *C. elegans* germ lineage. Nature 551: 629–633. https://doi.org/10.1038/nature24620

Boxem, M., D. G. Srinivasan, and S. van den Heuvel, 1999 The *Caenorhabditis elegans* gene *ncc-1* encodes a cdc2-related kinase required for M phase in meiotic and mitotic cell divisions, but not for S phase. Development 126: 2227–2239.

Burrows, A. E., B. K. Sceurman, M. E. Kosinski, C. T. Richie, P. L. Sadler *et al.*, 2006 The *C. elegans* Myt1 ortholog is required for the proper timing of oocyte maturation. Development 133: 697–709. https://doi.org/10.1242/dev.02241

Chalfie, M., Y. Tu, G. Euskirchen, W. W. Ward, and D. C. Prasher, 1994 Green fluorescent protein as a marker for gene expression. Science 263: 802–805. https://doi.org/10.1126/science.8303295

Cheng, K. C., R. Klancer, A. Singson, and G. Seydoux, 2009 Regulation of MBK-2/DYRK by CDK-1 and the pseudophosphatases EGG-4 and EGG-5 during the oocyte-to-embryo transition. Cell 139: 560–572. https://doi.org/10.1016/j.cell.2009.08.047

Crittenden, S. L., D. S. Bernstein, J. L. Bachorik, B. E. Thompson, M. Gallegos *et al.*, 2002 A conserved RNA-binding protein controls germline stem cells in *Caenorhabditis elegans*. Nature 417: 660–663. https://doi.org/10.1038/nature754

Cross, F. R., L. Schroeder, and J. M. Bean, 2007 Phosphorylation of the Sic1 inhibitor of B-type cyclins in *Saccharomyces cerevisiae* is not essential but contributes to cell cycle robustness. Genetics 176: 1541–1555. https://doi.org/10.1534/genetics.107.073494

Csizmok, V., M. Montecchio, H. Lin, M. Tyers, M. Sunnerhagen *et al.*, 2018 Multivalent interactions with Fbw7 and Pin1 facilitate recognition of c-Jun by the SCF^{Fbw7} ubiquitin ligase. Structure 26: 28–39.e2. https://doi.org/10.1016/j.str.2017.11.003

Cuevas, E., A. Rybak-Wolf, A. M. Rhode, D. T. T. Nguyen, and F. G. Wulczyn, 2015 Lin41/Trim71 is essential for mouse development and specifically expressed in postnatal ependymal cells of the brain. Front. Cell Dev. Biol. 3: 20. https://doi.org/10.3389/fcell.2015.00020

de la Cova, C., and I. Greenwald, 2012 SEL-10/Fbw7-dependent negative feedback regulation of LIN-45/Braf signaling in *C. elegans* via a conserved phosphodegron. Genes Dev. 26: 2524–2535. https://doi.org/10.1101/gad.203703.112

Del Rio-Albrechtsen, T., K. Kiontke, S. Y. Chiou, and D. H. Fitch, 2006 Novel gain-of-function alleles demonstrate a role for the heterochronic gene *lin-41* in *C. elegans* male tail tip morphogenesis. Dev. Biol. 297: 74–86. https://doi.org/10.1016/j.ydbio.2006.04.472

Dephoure, N., K. L. Gould, S. P. Gygi, and D. R. Kellogg, 2013 Mapping and analysis of phosphorylation sites: a quick guide for cell biologists. Mol. Biol. Cell 24: 535–542. https://doi.org/10.1091/mbc.e12-09-0677

Deshaies, R. J., and J. E. Ferrell, 2001 Multisite phosphorylation and the countdown to S phase. Cell 107: 819–822. https://doi.org/10.1016/S0092-8674(01)00620-1

Detwiler, M. R., M. Reuben, X. Li, E. Rogers, and R. Lin, 2001 Two zinc finger proteins, OMA-1 and OMA-2, are redundantly required for oocyte maturation in *C. elegans*. Dev. Cell 1: 187–199. https://doi.org/10.1016/S1534-5807(01)00026-0

Dickinson, D. J., J. D. Ward, D. J. Reiner, and B. Goldstein, 2013 Engineering the *Caenorhabditis elegans* genome using Cas9-triggered homologous recombination. Nat. Methods 10: 1028–1034. https://doi.org/10.1038/nmeth.2641

Dickinson, D. J., A. M. Pani, J. K. Heppert, C. D. Higgins, and B. Goldstein, 2015 Streamlined genome engineering with a self-excising drug selection cassette. Genetics 200: 1035–1049. https://doi.org/10.1534/genetics.115.178335

Doh, J. H., Y. Jung, V. Reinke, and M. H. Lee, 2013 *C. elegans* RNA-binding protein GLD-1 recognizes its multiple targets using sequence, context, and structural information to repress translation. Worm 2: e26548. https://doi.org/10.4161/worm.26548

Draper, B. W., C. C. Mello, B. Bowerman, J. Hardin, and J. R. Priess, 1996 MEX-3 is a KH domain protein that regulates blastomere identity in early *C. elegans* embryos. Cell 87: 205–216. https://doi.org/10.1016/S0092-8674(00)81339-2

Du, Z., F. He, Z. Yu, B. Bowerman, and Z. Bao, 2015 E3 ubiquitin ligases promote progression of differentiation during *C. elegans* embryogenesis. Dev. Biol. 398: 267–279. https://doi.org/10.1016/j.ydbio.2014.12.009

Dunphy, W. G., L. Brizuela, D. Beach, and J. Newport, 1988 The *Xenopus* cdc2 protein is a component of MPF, a cytoplasmic regulator of mitosis. Cell 54: 423–431. https://doi.org/10.1016/0092-8674(88)90205-X

Ellis, R. E., and J. Kimble, 1995 The *fog-3* gene and regulation of cell fate in the germ line of *Caenorhabditis elegans*. Genetics 139: 561–577.

Esposito, D., M. G. Koliopoulos, and K. Rittinger, 2017 Structural determinants of TRIM protein function. Biochem. Soc. Trans. 45: 183–191. https://doi.org/10.1042/BST20160325

Farley, B. M., and S. P. Ryder, 2012 POS-1 and GLD-1 repress *glp-1* translation through a conserved binding-site cluster. Mol. Biol. Cell 23: 4473–4483. https://doi.org/10.1091/mbc.e12-03-0216

Feldman, R. M., C. C. Correll, K. B. Kaplan, and R. J. Deshaies, 1997 A complex of Cdc4p, Skp1p, and Cdc53/cullin catalyzes ubiquitination of the phosphorylated CDK inhibitor Sic1p. Cell 91: 221–230. https://doi.org/10.1016/S0092-8674(00)80404-3

Fox, P. M., V. E. Vought, M. Hanazawa, M. H. Lee, E. M. Maine *et al.*, 2011 Cyclin E and CDK-2 regulate proliferative cell fate and cell cycle progression in the *C. elegans* germline. Development 138: 2223–2234. https://doi.org/10.1242/dev.059535

Francis, R., E. Maine, and T. Schedl, 1995a Analysis of the multiple roles of *gld-1* in germline development: interactions with the sex determination cascade and the *glp-1* signaling pathway. Genetics 139: 607–630.

Francis, R., M. K. Barton, J. Kimble, and T. Schedl, 1995b *gld-1*, a tumor suppressor gene required for oocyte development in *Caenorhabditis elegans*. Genetics 139: 579–606.

Frank-Vaillant, M., C. Jessus, R. Ozon, J. L. Maller, and O. Haccard, 1999 Two distinct mechanisms control the accumulation of cyclin B1 and Mos in *Xenopus* oocytes in response to progesterone. Mol. Biol. Cell 10: 3279–3288. https://doi.org/10.1091/mbc.10.10.3279

Furuta, T., S. Tuck, J. Kirchner, B. Koch, R. Auty *et al.*, 2000 EMB-30: an APC4 homologue required for metaphase-to-anaphase transitions during meiosis and mitosis in *Caenorhabditis elegans*. Mol. Biol. Cell 11: 1401–1419. https://doi.org/10.1091/mbc.11.4.1401

Gautier, J., C. Norbury, M. Lohka, P. Nurse, and J. Maller, 1988 Purified maturation-promoting factor contains the product of a *Xenopus* homolog of the fission yeast cell cycle control gene cdc2+. Cell 54: 433–439. https://doi.org/10.1016/0092-8674(88)90206-1

Gautier, J., J. Minshull, M. Lohka, M. Glotzer, T. Hunt *et al.*, 1990 Cyclin is a component of maturation-promoting factor from *Xenopus*. Cell 60: 487–494. https://doi.org/10.1016/0092-8674(90)90599-A

Gomes, J. E., S. E. Encalada, K. A. Swan, C. A. Shelton, J. C. Carter *et al.*, 2001 The maternal gene *spn-4* encodes a predicted RRM protein required for mitotic spindle orientation and cell fate patterning in early *C. elegans* embryos. Development 128: 4301–4314.

Gouw, M., S. Michael, H. Sámano-Sánchez, M. Kumar, A. Zeke *et al.*, 2018 The eukaryotic linear motif resource - 2018 update. Nucleic Acids Res. 46: D428–D434. https://doi.org/10.1093/nar/gkx1077

Govindan, J. A., H. Cheng, J. E. Harris, and D. Greenstein, 2006 Galphao/i and Galphas signaling function in parallel with the MSP/Eph receptor to control meiotic diapause in *C. elegans*. Curr. Biol. 16: 1257–1268. https://doi.org/10.1016/j.cub.2006.05.020

Govindan, J. A., S. Nadarajan, S. Kim, T. A. Starich, and D. Greenstein, 2009 Somatic cAMP signaling regulates MSP-dependent oocyte growth and meiotic maturation in *C. elegans*. Development 136: 2211–2221. https://doi.org/10.1242/dev.034595

Grant, B., and D. Hirsh, 1999 Receptor-mediated endocytosis in the *Caenorhabditis elegans* oocyte. Mol. Biol. Cell 10: 4311–4326. https://doi.org/10.1091/mbc.10.12.4311

Guven-Ozkan, T., S. M. Robertson, Y. Nishi, and R. Lin, 2010 *zif-1* translational repression defines a second, mutually exclusive OMA function in germline transcriptional repression. Development 137: 3373–3382. https://doi.org/10.1242/dev.055327

Guven-Ozkan, T., Y. Nishi, S. M. Robertson, and R. Lin, 2008 Global transcriptional repression in *C. elegans* germline precursors by regulated sequestration of TAF-4. Cell 135: 149–160. https://doi.org/10.1016/j.cell.2008.07.040

Haccard, O., and C. Jessus, 2006a Redundant pathways for Cdc2 activation in *Xenopus* oocyte: either cyclin B or Mos synthesis. EMBO Rep. 7: 321–325. https://doi.org/10.1038/sj.embor.7400611

Haccard, O., and C. Jessus, 2006b Oocyte maturation, Mos and cyclins–a mater of synthesis: two functionally redundant ways to induce meiotic maturation. Cell Cycle 5: 1152–1159. https://doi.org/10.4161/cc.5.11.2800

Hansen, D., and T. Schedl, 2013 Stem cell proliferation *vs.* meiotic fate decision in *Caenorhabditis elegans*. Adv. Exp. Med. Biol. 757: 71–99. https://doi.org/10.1007/978-1-4614-4015-4_4

Hansen, D., L. Wilson-Berry, T. Dang, and T. Schedl, 2004 Control of the proliferation *vs.* meiotic development decision in the *C. elegans* germline through regulation of GLD-1 protein accumulation. Development 131: 93–104. https://doi.org/10.1242/dev.00916

Harris, D. T., and H. R. Horvitz, 2011 MAB-10/NAB acts with LIN-29/EGR to regulate terminal differentiation and the transition from larva to adult in *C. elegans*. Development 138: 4051–4062. https://doi.org/10.1242/dev.065417

Hasegawa, E., T. Karashima, E. Sumiyoshi, and M. Yamamoto, 2006 *C. elegans* CPB-3 interacts with DAZ-1 and functions in multiple steps in germline development. Dev. Biol. 295: 689–699. https://doi.org/10.1016/j.ydbio.2006.04.002

Huelgas-Morales, G., and D. Greenstein, 2017 Control of oocyte meiotic maturation in *C. elegans*. Semin. Cell Dev. Biol. (in press). https://doi.org/10.1016/j.semcdb.2017.12.005

Hopkins, M., J. J. Tyson, and B. Novák, 2017 Cell-cycle transitions: a common role for stoichiometric inhibitors. Mol. Biol. Cell 28: 3437–3446. https://doi.org/10.1091/mbc.e17-06-0349

Hsu, J. Y., Z. W. Sun, X. Li, M. Reuben, K. Tatchell *et al.*, 2000 Mitotic phosphorylation of histone H3 is governed by

Ipl1/aurora kinase and Glc7/PP1 phosphatase in budding yeast and nematodes. Cell 102: 279–291. https://doi.org/10.1016/S0092-8674(00)00034-9

Hubbard, E. J., G. Wu, J. Kitajewski, and I. Greenwald, 1997 *sel-10*, a negative regulator of *lin-12* activity in *Caenorhabditis elegans*, encodes a member of the CDC4 family of proteins. Genes Dev. 11: 3182–3193. https://doi.org/10.1101/gad.11.23.3182

Ikeda, K., and S. Inoue, 2012 TRIM proteins as RING finger E3 ubiquitin ligases. Adv. Exp. Med. Biol. 770: 27–37. https://doi.org/10.1007/978-1-4614-5398-7_3

Jan, E., C. K. Motzny, L. E. Graves, and E. B. Goodwin, 1999 The STAR protein, GLD-1, is a translational regulator of sexual identity in *Caenorhabditis elegans*. EMBO J. 18: 258–269. https://doi.org/10.1093/emboj/18.1.258

Jeong, J., J. M. Verheyden, and J. Kimble, 2011 Cyclin E and Cdk2 control GLD-1, the mitosis/meiosis decision, and germline stem cells in *Caenorhabditis elegans*. PLoS Genet. 7: e1001348. https://doi.org/10.1371/journal.pgen.1001348

Jones, A. R., and T. Schedl, 1995 Mutations in *gld-1*, a female germ cell-specific tumor suppressor gene in *Caenorhabditis elegans*, affect a conserved domain also found in Src-associated protein Sam68. Genes Dev. 9: 1491–1504. https://doi.org/10.1101/gad.9.12.1491

Jones, A. R., R. Francis, and T. Schedl, 1996 GLD-1, a cytoplasmic protein essential for oocyte differentiation, shows stage- and sex-specific expression during *Caenorhabditis elegans* germline development. Dev. Biol. 180: 165–183. https://doi.org/10.1006/dbio.1996.0293

Jungkamp, A. C., M. Stoeckius, D. Mecenas, D. Grün, G. Mastrobuoni *et al.*, 2011 *In vivo* and transcriptome-wide identification of RNA binding protein target sites. Mol. Cell 44: 828–840. https://doi.org/10.1016/j.molcel.2011.11.009

Kadyk, L. C., and J. Kimble, 1998 Genetic regulation of entry into meiosis in *Caenorhabditis elegans*. Development 125: 1803–1813.

Kapelle, W. S., and V. Reinke, 2011 *C. elegans meg-1* and *meg-2* differentially interact with *nanos* family members to either promote or inhibit germ cell proliferation and survival. Genesis 49: 380–391. https://doi.org/10.1002/dvg.20726

Killian, D. J., E. Harvey, P. Johnson, M. Otori, S. Mitani *et al.*, 2008 SKR-1, a homolog of Skp1 and a member of the SCF (SEL-10) complex, regulates sex-determination and LIN-12/Notch signaling in *C. elegans*. Dev. Biol. 322: 322–331. https://doi.org/10.1016/j.ydbio.2008.07.035

Kipreos, E. T., L. E. Lander, J. P. Wing, W. W. He, and E. M. Hedgecock, 1996 *cul-1* is required for cell cycle exit in *C. elegans* and identifies a novel gene family. Cell 85: 829–839. https://doi.org/10.1016/S0092-8674(00)81267-2

Kishimoto, T., 2015 Entry into mitosis: a solution to the decades-long enigma of MPF. Chromosoma 124: 417–428. https://doi.org/10.1007/s00412-015-0508-y

Kisielnicka, E., R. Minasaki, and C. R. Eckmann, 2018 MAPK signaling couples SCF-mediated degradation of translational regulators to oocyte meiotic progression. Proc. Natl. Acad. Sci. USA 115: E2772–E2781. https://doi.org/10.1073/pnas.1715439115

Kobayashi, H., J. Minshull, C. Ford, R. Golsteyn, R. Poon *et al.*, 1991 On the synthesis and destruction of A- and B-type cyclins during oogenesis and meiotic maturation in *Xenopus laevis*. J. Cell Biol. 114: 755–765. https://doi.org/10.1083/jcb.114.4.755

Koepp, D. M., L. K. Schaefer, X. Ye, K. Keyomarsi, C. Chu *et al.*, 2001 Phosphorylation-dependent ubiquitination of cyclin E by the SCF^{Fbw7} ubiquitin ligase. Science 294: 173–177. https://doi.org/10.1126/science.1065203

Kõivomägi, M., E. Valk, R. Venta, A. Iofik, M. Lepiku *et al.*, 2011 Cascades of multisite phosphorylation control Sic1 destruction at the onset of S phase. Nature 480: 128–131. https://doi.org/10.1038/nature10560

Kornbluth, S., B. Sebastian, T. Hunter, and J. Newport, 1994 Membrane localization of the kinase which phosphorylates p34cdc2 on threonine 14. Mol. Biol. Cell 5: 273–282. https://doi.org/10.1091/mbc.5.3.273

Kosinski, M., K. McDonald, J. Schwartz, I. Yamamoto, and D. Greenstein, 2005 *C. elegans* sperm bud vesicles to deliver a meiotic maturation signal to distant oocytes. Development 132: 3357–3369. https://doi.org/10.1242/dev.01916

Kumagai, A., and W. G. Dunphy, 1996 Purification and molecular cloning of Plx1, a Cdc25-regulatory kinase from *Xenopus* egg extracts. Science 273: 1377–1380. https://doi.org/10.1126/science.273.5280.1377

Kumari, P., F. Aeschimann, D. Gaidatzis, J. J. Keusch, P. Ghosh *et al.*, 2018 Evolutionary plasticity of the NHL domain underlies distinct solutions to RNA recognition. Nat. Commun. 9: 1549. https://doi.org/10.1038/s41467-018-03920-7

Kumsta, C., and M. Hansen, 2012 *C. elegans rrf-1* mutations maintain RNAi efficiency in the soma in addition to the germline. PLoS One 7: e35428. https://doi.org/10.1371/journal.pone.0035428

Leacock, S. W., and V. Reinke, 2008 MEG-1 and MEG-2 are embryo-specific P-granule components required for germline development in *Caenorhabditis elegans*. Genetics 178: 295–306. https://doi.org/10.1534/genetics.107.080218

Lee, M. H., and T. Schedl, 2001 Identification of *in vivo* mRNA targets of GLD-1, a maxi-KH motif containing protein required for *C. elegans* germ cell development. Genes Dev. 15: 2408–2420. https://doi.org/10.1101/gad.915901

Lee, M. H., and T. Schedl, 2004 Translation repression by GLD-1 protects its mRNA targets from nonsense-mediated mRNA decay in *C. elegans*. Genes Dev. 18: 1047–1059. https://doi.org/10.1101/gad.1188404

Lee, M. H., and T. Schedl, 2010 *C. elegans* star proteins, GLD-1 and ASD-2, regulate specific RNA targets to control development. Adv. Exp. Med. Biol. 693: 106–122. https://doi.org/10.1007/978-1-4419-7005-3_8

Lee, M. H., M. Ohmachi, S. Arur, S. Nayak, R. Francis *et al.*, 2007 Multiple functions and dynamic activation of MPK-1 extracellular signal-regulated kinase signaling in *Caenorhabditis elegans* germline development. Genetics 177: 2039–2062. https://doi.org/10.1534/genetics.107.081356

Li, W., L. R. DeBella, T. Guven-Ozkan, R. Lin, and L. S. Rose, 2009 An eIF4E-binding protein regulates katanin protein levels in *C. elegans* embryos. J. Cell Biol. 187: 33–42. https://doi.org/10.1083/jcb.200903003

Lin, R., 2003 A gain-of-function mutation in *oma-1*, a *C. elegans* gene required for oocyte maturation, results in delayed degradation of maternal proteins and embryonic lethality. Dev. Biol. 258: 226–239. https://doi.org/10.1016/S0012-1606(03)00119-2

Loedige, I., D. Gaidatzis, R. Sack, G. Meister, and W. Filipowicz, 2013 The mammalian TRIM-NHL protein TRIM71/LIN-41 is a repressor of mRNA function. Nucleic Acids Res. 41: 518–532. https://doi.org/10.1093/nar/gks1032

Loedige, I., L. Jakob, T. Treiber, D. Ray, M. Stotz *et al.*, 2015 The crystal structure of the NHL domain in complex with RNA reveals the molecular basis of *Drosophila brain-tumor*-mediated gene regulation. Cell Rep. 13: 1206–1220. https://doi.org/10.1016/j.celrep.2015.09.068

Lohka, M. J., M. K. Hayes, and J. L. Maller, 1988 Purification of maturation-promoting factor, an intracellular regulator of early mitotic events. Proc. Natl. Acad. Sci. USA 85: 3009–3013. https://doi.org/10.1073/pnas.85.9.3009

Lucas, X., and A. Ciulli, 2017 Recognition of substrate degrons by E3 ubiquitin ligases and modulation by small-molecule mimicry strategies. Curr. Opin. Struct. Biol. 44: 101–110. https://doi.org/10.1016/j.sbi.2016.12.015

Maller Schulman, B. R., X. Liang, C. Stahlhut, C. DelConte, G. Stefani *et al.*, 2008 The *let-7* microRNA target gene, *Mlin41/Trim71* is required for mouse embryonic survival and neural tube closure. Cell Cycle 7: 3935–3942. https://doi.org/10.4161/cc.7.24.7397

Masui, Y., 2001 From oocyte maturation to the *in vitro* cell cycle: the history of discoveries of Maturation-Promoting Factor (MPF) and Cytostatic Factor (CSF). Differentiation 69: 1–17. https://doi.org/10.1046/j.1432-0436.2001.690101.x

Masui, Y., and C. L. Markert, 1971 Cytoplasmic control of nuclear behavior during meiotic maturation of frog oocytes. J. Exp. Zool. 177: 129–145. https://doi.org/10.1002/jez.1401770202

Matsuura, R., T. Ashikawa, Y. Nozaki, and D. Kitagawa, 2016 LIN-41 inactivation leads to delayed centrosome elimination and abnormal chromosome behavior during female meiosis in *Caenorhabditis elegans*. Mol. Biol. Cell 27: 799–811. https://doi.org/10.1091/mbc.e15-10-0713

McCarter, J., B. Bartlett, T. Dang, and T. Schedl, 1999 On the control of oocyte meiotic maturation and ovulation in *Caenorhabditis elegans*. Dev. Biol. 205: 111–128. https://doi.org/10.1006/dbio.1998.9109

McNally, K., A. Audhya, K. Oegema, and F. J. McNally, 2006 Katanin controls mitotic and meiotic spindle length. J. Cell Biol. 175: 881–891. https://doi.org/10.1083/jcb.200608117

Merritt, C., D. Rasoloson, D. Ko, and G. Seydoux, 2008 3′ UTRs are the primary regulators of gene expression in the *C. elegans* germline. Curr. Biol. 18: 1476–1482. https://doi.org/10.1016/j.cub.2008.08.013

Miller, M. A., V. Q. Nguyen, M. H. Lee, M. Kosinski, T. Schedl *et al.*, 2001 A sperm cytoskeletal protein that signals oocyte meiotic maturation and ovulation. Science 291: 2144–2147. https://doi.org/10.1126/science.1057586

Minshull, J., A. Murray, A. Colman, and T. Hunt, 1991 *Xenopus* oocyte maturation does not require new cyclin synthesis. J. Cell Biol. 114: 767–772. https://doi.org/10.1083/jcb.114.4.767

Mitschka, S., T. Ulas, T. Goller, K. Schneider, A. Egert *et al.*, 2015 Co-existence of intact stemness and priming of neural differentiation programs in mES cells lacking Trim71. Sci. Rep. 5: 11126. https://doi.org/10.1038/srep11126

Mohammad, A., K. Vanden Broek, C. Wang, A. Daryabeigi, V. Jantsch *et al.*, 2018 Initiation of meiotic development is controlled by three posttranscriptional pathways in *Caenorhabditis elegans*. Genetics 209: 1197–1224. https://doi.org/10.1534/genetics.118.300985

Mootz, D., D. M. Ho, and C. P. Hunter, 2004 The STAR/Maxi-KH domain protein GLD-1 mediates a developmental switch in the translational control of *C. elegans* PAL-1. Development 131: 3263–3272. https://doi.org/10.1242/dev.01196

Mueller, P. R., T. R. Coleman, and W. G. Dunphy, 1995 Cell cycle regulation of a *Xenopus* Wee1-like kinase. Mol Biol Cell 6: 119–134.

Nash, P., X. Tang, S. Orlicky, Q. Chen, F. B. Gertler *et al.*, 2001 Multisite phosphorylation of a CDK inhibitor sets a threshold for the onset of DNA replication. Nature 414: 514–521. https://doi.org/10.1038/35107009

Nayak, S., F. E. Santiago, H. Jin, D. Lin, T. Schedl *et al.*, 2002 The *Caenorhabditis elegans* Skp1-related gene family: diverse functions in cell proliferation, morphogenesis, and meiosis. Curr. Biol. 12: 277–287. https://doi.org/10.1016/S0960-9822(02)00682-6

Nebreda, A. R., J. V. Gannon, and T. Hunt, 1995 Newly synthesized protein(s) must associate with p34cdc2 to activate MAP kinase and MPF during progesterone-induced maturation of *Xenopus* oocytes. EMBO J. 14: 5597–5607. https://doi.org/10.1002/j.1460-2075.1995.tb00247.x

Nishi, Y., and R. Lin, 2005 DYRK2 and GSK-3 phosphorylate and promote the timely degradation of OMA-1, a key regulator of the oocyte-to-embryo transition in *C. elegans*. Dev. Biol. 288: 139–149. https://doi.org/10.1016/j.ydbio.2005.09.053

Nugroho, T. T., and M. D. Mendenhall, 1994 An inhibitor of yeast cyclin-dependent protein kinase plays an important role in ensuring the genomic integrity of daughter cells. Mol. Cell. Biol. 14: 3320–3328. https://doi.org/10.1128/MCB.14.5.3320

Nurse, P., 1990 Universal control mechanism regulating onset of M-phase. Nature 344: 503–508. https://doi.org/10.1038/344503a0

Nyström, J., Z. Z. Shen, M. Aili, A. J. Flemming, A. Leroi *et al.*, 2002 Increased or decreased levels of *Caenorhabditis elegans lon-3*, a gene encoding a collagen, cause reciprocal changes in body length. Genetics 161: 83–97.

O'Farrell, P. H., 2001 Triggering the all-or-nothing switch into mitosis. Trends Cell Biol. 11: 512–519. https://doi.org/10.1016/S0962-8924(01)02142-0

Ogura, K., N. Kishimoto, S. Mitani, K. Gengyo-Ando, and Y. Kohara, 2003 Translational control of maternal *glp-1* mRNA by POS-1 and its interacting protein SPN-4 in *Caenorhabditis elegans*. Development 130: 2495–2503. https://doi.org/10.1242/dev.00469

Parry, J. M., N. V. Velarde, A. J. Lefkovith, M. H. Zegarek, J. S. Hang *et al.*, 2009 EGG-4 and EGG-5 link events of the oocyte-to-embryo transition with meiotic progression in *C. elegans*. Curr. Biol. 19: 1752–1757. https://doi.org/10.1016/j.cub.2009.09.015

Peel, N., M. Dougherty, J. Goeres, Y. Liu, and K. F. O'Connell, 2012 The *C. elegans* F-box proteins LIN-23 and SEL-10 antagonize centrosome duplication by regulating ZYG-1 levels. J. Cell Sci. 125: 3535–3544. https://doi.org/10.1242/jcs.097105

Pellettieri, J., V. Reinke, S. K. Kim, and G. Seydoux, 2003 Coordinate activation of maternal protein degradation during the egg-to-embryo transition in *C. elegans*. Dev. Cell 5: 451–462. https://doi.org/10.1016/S1534-5807(03)00231-4

Reinhart, B. J., F. J. Slack, M. Basson, A. E. Pasquinelli, J. C. Bettinger *et al.*, 2000 The 21-nucleotide *let-7* RNA regulates developmental timing in *Caenorhabditis elegans*. Nature 403: 901–906. https://doi.org/10.1038/35002607

Robertson, S., and R. Lin, 2015 The maternal-to-zygotic transition in *C. elegans*. Curr. Top. Dev. Biol. 113: 1–42. https://doi.org/10.1016/bs.ctdb.2015.06.001

Rose, K. L., V. P. Winfrey, L. H. Hoffman, D. H. Hall, T. Furuta *et al.*, 1997 The POU gene *ceh-18* promotes gonadal sheath cell differentiation and function required for meiotic maturation and ovulation in *Caenorhabditis elegans*. Dev. Biol. 192: 59–77. https://doi.org/10.1006/dbio.1997.8728

Rougvie, A. E., and E. G. Moss, 2013 Developmental transitions in *C. elegans* larval stages. Curr. Top. Dev. Biol. 105: 153–180. https://doi.org/10.1016/B978-0-12-396968-2.00006-3

Rybak, A., H. Fuchs, K. Hadian, L. Smirnova, E. A. Wulczyn *et al.*, 2009 The *let-7* target gene mouse *lin-41* is a stem cell specific E3 ubiquitin ligase for the miRNA pathway protein Ago2. Nat. Cell Biol. 11: 1411–1420. https://doi.org/10.1038/ncb1987

Scheckel, C., D. Gaidatzis, J. E. Wright, and R. Ciosk, 2012 Genome-wide analysis of GLD-1-mediated mRNA regulation suggests a role in mRNA storage. PLoS Genet. 8: e1002742. https://doi.org/10.1371/journal.pgen.1002742

Schedl, T., and J. Kimble, 1988 *fog-2*, a germline-specific sex determination gene required for hermaphrodite spermatogenesis in *Caenorhabditis elegans*. Genetics 119: 43–61.

Schumacher, B., M. Hanazawa, M. H. Lee, S. Nayak, K. Volkmann *et al.*, 2005 Translational repression of *C. elegans* p53 by GLD-1 regulates DNA damage-induced apoptosis. Cell 120: 357–368. https://doi.org/10.1016/j.cell.2004.12.009

Shaner, N. C., G. G. Lambert, A. Chammas, Y. Ni, P. J. Cranfill *et al.*, 2013 A bright monomeric green fluorescent protein derived from *Branchiostoma lanceolatum*. Nat. Methods 10: 407–409. https://doi.org/10.1038/nmeth.2413

Shirayama, M., M. C. Soto, T. Ishidate, S. Kim, K. Nakamura *et al.*, 2006 The conserved kinases CDK-1, GSK-3, KIN-19, and MBK-

2 promote OMA-1 destruction to regulate the oocyte-to-embryo transition in *C. elegans*. Curr. Biol. 16: 47–55. https://doi.org/10.1016/j.cub.2005.11.070

Schwob, E., T. Böhm, M. D. Mendenhall, and K. Nasmyth, 1994 The B-type cyclin kinase inhibitor p40^{SIC1} controls the G1 to S transition in *S. cerevisae*. Cell 79: 233–244. https://doi.org/10.1016/0092-8674(94)90193-7

Sijen, T., J. Fleenor, F. Simmer, K. L. Thijssen, S. Parrish *et al.*, 2001 On the role of RNA amplification in dsRNA-triggered gene silencing. Cell 107: 465–476. https://doi.org/10.1016/S0092-8674(01)00576-1

Slack, F. J., and G. Ruvkun, 1998 A novel repeat domain that is often associated with RING finger and B-box motifs. Trends Biochem. Sci. 23: 474–475. https://doi.org/10.1016/S0968-0004(98)01299-7

Slack, F. J., M. Basson, Z. Liu, V. Ambros, H. R. Horvitz *et al.*, 2000 The *lin-41* RBCC gene acts in the *C. elegans* heterochronic pathway between the *let*-7 regulatory RNA and the LIN-29 transcription factor. Mol. Cell 5: 659–669. https://doi.org/10.1016/S1097-2765(00)80245-2

Sonneville, R., M. Querenet, A. Craig, A. Gartner, and J. J. Blow, 2012 The dynamics of replication licensing in live *Caenorhabditis elegans* embryos. J. Cell Biol. 196: 233–246. https://doi.org/10.1083/jcb.201110080

Spike, C. A., D. Coetzee, C. Eichten, X. Wang, D. Hansen *et al.*, 2014a The TRIM-NHL protein LIN-41 and the OMA RNA-binding proteins antagonistically control the prophase-to-metaphase transition and growth of *Caenorhabditis elegans* oocytes. Genetics 198: 1535–1558. https://doi.org/10.1534/genetics.114.168831

Spike, C. A., D. Coetzee, Y. Nishi, T. Guven-Ozkan, M. Oldenbroek *et al.*, 2014b Translational control of the oogenic program by components of OMA ribonucleoprotein particles in *Caenorhabditis elegans*. Genetics 198: 1513–1533. https://doi.org/10.1534/genetics.114.168823

Stitzel, M. L., J. Pellettieri, and G. Seydoux, 2006 The *C. elegans* DYRK kinase MBK-2 marks oocyte proteins for degradation in response to meiotic maturation. Curr. Biol. 16: 56–62. https://doi.org/10.1016/j.cub.2005.11.063

Stitzel, M. L., K. C. Cheng, and G. Seydoux, 2007 Regulation of MBK-2/Dyrk kinase by dynamic cortical anchoring during the oocyte-to-zygote transition. Curr. Biol. 17: 1545–1554. https://doi.org/10.1016/j.cub.2007.08.049

Stoeckius, M., D. Grün, M. Kirchner, S. Ayoub, F. Torti *et al.*, 2014 Global characterization of the oocyte-to-embryo transition in *Caenorhabditis elegans* uncovers a novel mRNA clearance mechanism. EMBO J. 33: 1751–1766. https://doi.org/10.15252/embj.201488769

Strohmaier, H., C. H. Spruck, P. Kaiser, K.-A. Won, O. Sangfelt *et al.*, 2001 Human F-box protein hCdc4 targets cyclin E for proteolysis and is mutated in a breast cancer cell line. Nature 413: 316–322. https://doi.org/10.1038/35095076

Sundaram, M., and I. Greenwald, 1993 Suppressors of a *lin-12* hypomorph define genes that interact with both *lin-12* and *glp-1* in *Caenorhabditis elegans*. Genetics 135: 765–783.

Suzuki, Y., G. A. Morris, M. Han, and W. B. Wood, 2002 A cuticle collagen encoded by the *lon-3* gene may be a target of TGF-beta signaling in determining *Caenorhabditis elegans* body shape. Genetics 162: 1631–1639.

Svoboda, P., H. Fulka, and R. Malik, 2017 Clearance of parental products. Adv. Exp. Med. Biol. 953: 489–535. https://doi.org/10.1007/978-3-319-46095-6_10

Timmons, L., and A. Fire, 1998 Specific interference by ingested dsRNA. Nature 395: 854. https://doi.org/10.1038/27579

Tocchini, C., J. J. Keusch, S. B. Miller, S. Finger, H. Gut *et al.*, 2014 The TRIM-NHL protein LIN-41 controls the onset of developmental plasticity in *Caenorhabditis elegans*. PLoS Genet. 10: e1004533. https://doi.org/10.1371/journal.pgen.1004533

Tsukamoto, T., M. D. Gearhart, C. A. Spike, G. Huelgas-Morales, M. Mews *et al.*, 2017 LIN-41 and OMA ribonucleoprotein complexes mediate a translational repression-to-activation switch controlling oocyte meiotic maturation and the oocyte-to-embryo transition in *Caenorhabditis elegans*. Genetics 206: 2007–2039. https://doi.org/10.1534/genetics.117.203174

Ubersax, J. A., E. L. Woodbury, P. N. Quang, M. Paraz, J. D. Blethrow *et al.*, 2003 Targets of the cyclin-dependent kinase Cdk1. Nature 425: 859–864. https://doi.org/10.1038/nature02062

van der Voet, M., M. A. Lorson, D. G. Srinivasan, K. L. Bennett, and S. van den Heuvel, 2009 *C. elegans* mitotic cyclins have distinct as well as overlapping functions in chromosome segregation. Cell Cycle 8: 4091–4102. https://doi.org/10.4161/cc.8.24.10171

Verlhac, M. H., M. E. Terret, and L. Pintard, 2010 Control of the oocyte-to-embryo transition by the ubiquitin-proteolytic system in mouse and *C. elegans*. Curr. Opin. Cell Biol. 22: 758–763. https://doi.org/10.1016/j.ceb.2010.09.003

Verma, R., R. S. Annan, M. J. Huddleston, S. A. Carr, G. Reynard *et al.*, 1997 Phosphorylation of Sic1p by G_1 Cdk required for its degradation and entry into S phase. Science 278: 455–460. https://doi.org/10.1126/science.278.5337.455

Wang, J. T., J. Smith, B. C. Chen, H. Schmidt, D. Rasoloson *et al.*, 2014 Regulation of RNA granule dynamics by phosphorylation of serine-rich, intrinsically disordered proteins in *C. elegans*. eLife 3: e04591. https://doi.org/10.7554/eLife.04591

Welcker, M., and B. E. Clurman, 2008 FBW7 ubiquitin ligase: a tumour suppressor at the crossroads of cell division, growth and differentiation. Nat. Rev. Cancer 8: 83–93. https://doi.org/10.1038/nrc2290

Welcker, M., E. A. Larimore, J. Swanger, M. T. Bengoechea-Alonso, J. E. Grim *et al.*, 2013 Fbw7 dimerization determines the specificity and robustness of substrate degradation. Genes Dev. 27: 2531–2536. https://doi.org/10.1101/gad.229195.113

Wolke, U., E. A. Jezuit, and J. R. Priess, 2007 Actin-dependent cytoplasmic streaming in *C. elegans* oogenesis. Development 134: 2227–2236. https://doi.org/10.1242/dev.004952

Wright, J. E., D. Gaidatzis, M. Senften, B. M. Farley, E. Westhof *et al.*, 2011 A quantitative RNA code for mRNA target selection by the germline fate determinant GLD-1. EMBO J. 30: 533–545. https://doi.org/10.1038/emboj.2010.334

Worringer, K. A., T. A. Rand, Y. Hayashi, S. Sami, K. Takahashi *et al.*, 2014 The *let-7*/LIN-41 pathway regulates reprogramming to human induced pluripotent stem cells by controlling expression of prodifferentiation genes. Cell Stem Cell 14: 40–52. https://doi.org/10.1016/j.stem.2013.11.001

Yamanaka, A., M. Yada, H. Imaki, M. Koga, Y. Ohshima *et al.*, 2002 Multiple Skp1-related proteins in *Caenorhabditis elegans*: diverse patterns of interaction with Cullins and F-box proteins. Curr. Biol. 12: 267–275. https://doi.org/10.1016/S0960-9822(02)00657-7

Yang, X., K.-Y. Lau, V. Sevim, and C. Tang, 2013 Design principles of the yeast G1/S switch. PLoS Biol. 11: e1001673. https://doi.org/10.1371/journal.pbio.1001673

Communicating editor: V. Reinke